

Optimization of a Formula SAE Vehicle Intake Manifold

A Technical Report submitted to the Department of Mechanical and Aerospace Engineering

Presented to the Faculty of the School of Engineering and Applied Science

University of Virginia • Charlottesville, Virginia

In Partial Fulfillment of the Requirements for the Degree

Bachelor of Science, School of Engineering

Dani Bilali

Spring, 2023

Technical Project Team Members

Pallavi Kulkarni

Brett Mihovetz

Sunniva Nyhus

Billy Robic

On my honor as a University Student, I have neither given nor received unauthorized aid on this assignment as defined by the Honor Guidelines for Thesis-Related Assignments

Michael Momot, Department of Mechanical and Aerospace Engineering

Table of Contents

1. An Overview of Formula SAE.....	3
2. Introduction.....	6
3. Constraints Screening and Scoring.....	9
4. Material Selection.....	13
5. Restrictor Optimization.....	19
6. Plenum Optimization.....	25
7. Runner Optimization.....	30
8. Connections.....	38
a. Fasteners.....	38
b. Gaskets.....	41
9. Structural Analysis.....	47
10. Manufacturing Phase.....	48
a. 3D Printing.....	52
b. CNC Milling.....	58
c. Epoxy Application.....	61
d. Additional Components.....	64
11. Assembly and Initial testing.....	65
12. Tuning.....	66
13. Results/Conclusion.....	67
14. Appendices.....	70
15. References.....	80

An Overview of Formula SAE

Formula SAE (FSAE) is a collegiate engineering competition organized by the Society of Automotive Engineers (SAE) to provide students with an opportunity to design and build an open cockpit, open wheel (Formula-1) style race car. The vehicle, and everything that goes along with designing and building it, is judged by international motorsports professionals on many criteria which are shown in Table I.

Table I: Formula SAE Competition Scoring Sheet (*FSAE*, n.d.)

Static Events	
Design Event	150
Cost & Manufacturing Analysis Event	100
Presentation Event	75
Dynamic Events	
Acceleration Event	100
Skidpad Event	75
Autocross Event	125
Fuel Economy Event	100
Endurance Event	275
Total Points Possible	1,000

The design event is considered by many engineering students as the most important of all the events. It consists of an hour long interview with approximately 15 judges with expertise in a variety of categories. The students are scored on multiple aspects of the vehicle which can be seen in Table II.

Table II: FSAE Design Scoring Sheet (FSAE design score sheet, n.d.)

Category	Areas Covered	Score
Suspension ○ Design ○ Build ○ Refinement/Validation ○ Understanding	Tires, wheels, hubs, uprights, control arms, steering linkage, springs, dampers, anti-roll bars, geometry, kinematics, vehicle dynamics. Selection and use of materials.	____/25
Frame/Body/Aero ○ Design ○ Build ○ Refinement/Validation ○ Understanding	Primary structure/tub/tubing, body, and aerodynamic/ ductwork systems. Rigidity and stress-relief methods. Load analyses. Fasteners. Selection and use of materials.	____/25
Powertrain ○ Design ○ Build ○ Refinement/Validation ○ Understanding	Engine, transmission, clutch, final drive, differential, half-shafts, tripods, etc. Also peripherals, such as cooling, oiling, electronic engine controls. Fuels/lubricants selection. Selection and use of materials.	____/25
Cockpit/Controls/Brakes/Safety ○ Design ○ Build ○ Refinement/Validation ○ Understanding	Driver interfaces, seat, belts, steering wheel, steering column, control panel/dash, cockpit sizing & protection, driver comfort/ease of control, shifter, pedals, braking system. Is this car as safe as it can be? Selection and use of materials.	____/25
Systems Management/Integration ○ Packaging ○ Electronics/power mgmt ○ Team Organization ○ Analysis methods/tools	Design integration, plumbing/wiring, power management, schematics. Are sensitive items protected? Proper use of data? Do systems compliment another? Are progressive project management/ organization methods evident? Special communication tools utilized? What testing/development tools have been used or created?	____/20
Manufacturability/Serviceability	Ease of repair? Sub-systems accessibility, parts interchangeability, manufacturing complexity? Have fasteners been standardized? Are special tools required to diagnose/service vehicle?	____/15
Aesthetics/Style	Attractive overall appearance? Is car clean, reflective of professional work? Does car instill pride in team, or apologies?	____/ 5
Creativity	Will this car cause a rules change? Have the judges learned something new? On rare occasions, creative or innovative design may merit special points.	____/10

The other categories that are relevant to this senior design project include the cost and manufacturing analysis, along with all of the dynamic events. The cost and manufacturing analysis will play a key role in the teams decision making on material selection and methods of manufacturing. The dynamic events include skidpad, acceleration, autocross, and endurance.

Skidpad consists of two, 15 meter radius circles, that drivers complete a figure 8 around. This event is to evaluate the vehicle's steady state cornering capability which is mainly a reflection of the vehicle's suspension. The acceleration event is a 75-meter-long drag race and tests a car's acceleration capabilities which is directly related to engine power output, overall weight, aerodynamics, and suspension anti-features. Autocross tracks vary year to year, but they are essentially a scaled-down Formula-1 style track. This event evaluates the overall handling of the car through various radii corners, slaloms, and straights on the track. An image of the FSAE Autocross track layout at the 2019 competition in Brooklyn, Michigan can be seen in Figure 1.

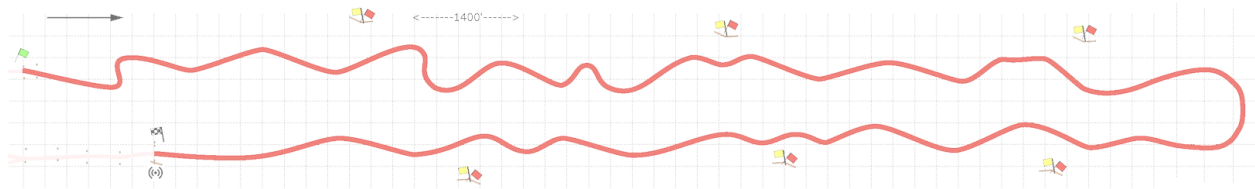


Figure 1. FSAE 2019 Autocross Track Layout (2019 FSAE Michigan, n.d.).

The final dynamic event, and arguably the most important, is the endurance event which not only tests if the vehicle can perform at a high performance level for a long period of time, but also tests the efficiency of the fuel system. An image of the 2019 FSAE Endurance track layout can be seen in Figure 2.

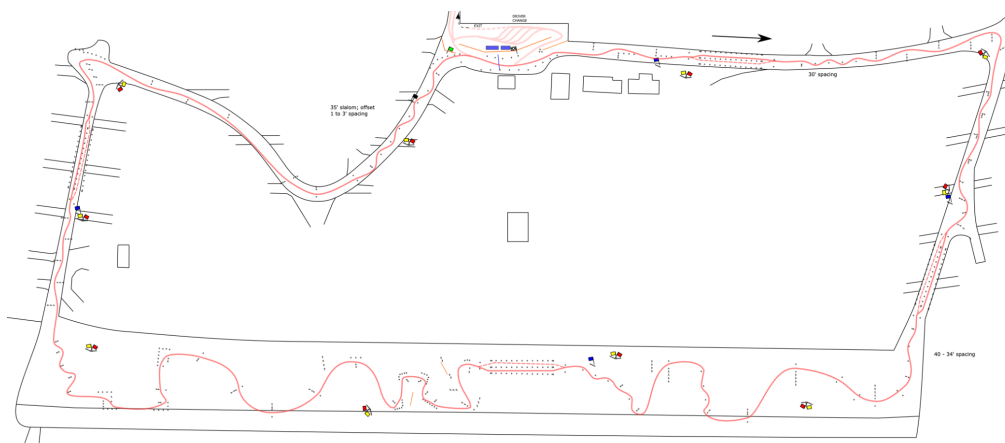


Figure 2. FSAE 2019 Endurance Track Layout (2019 FSAE Michigan, n.d.).

Introduction

The intake of a vehicle is crucial to its performance because it allows air to enter the engine. The oxygen in air is a crucial ingredient to the combustion process which provides power for a vehicle. The engine that will be used for this vehicle is a 600 cubic centimeter (cc) Yamaha R6 but has recently undergone a camshaft upgrade to optimize the engine for Formula SAE purposes. This is an important piece of information because the different camshafts will affect the engine timing which will in turn, affect the length of the runners and the design of the plenum. All teams are limited to a 700 cc motorcycle engine for the competition and there are multiple intake and exhaust restrictions to allow for fair competition at the collegiate level. The intake rules for the 2023 Formula SAE IC Competition can be seen below (*2023 FSAE rules VI*, n.d.).

1. All parts of the engine air system and fuel control, delivery and storage systems (including the throttle or carburetor, and the complete air intake system, including the air cleaner and any air boxes) must lie inside the Tire Surface Envelope F.1.14
2. Any portion of the air intake system that is less than 350 mm above the ground must be shielded from side or rear impacts by structure built per F.6.4 / F.7.5 as applicable.
3. The intake manifold must be securely attached to the engine block or cylinder head with brackets and mechanical fasteners:
 - a. Hose clamps, plastic ties, or safety wires do not meet this requirement.
 - b. The use of rubber bushings or hose is acceptable for creating and sealing air passages, but is not a structural attachment.

4. Threaded fasteners used to secure and/or seal the intake manifold must have a Positive Locking Mechanism, see T.8.3.
5. Intake systems with significant mass or cantilever from the cylinder head must be supported to prevent stress to the intake system.
 - a. Supports to the engine must be rigid.
 - b. Supports to the Chassis must incorporate some isolation to allow for engine movement and chassis flex.
6. All airflow to the engine(s) must pass through a single circular restrictor placed in the intake system.
7. The only allowed sequence of components are the following:
 - a. For naturally aspirated engines, the sequence must be: throttle body, restrictor, and engine.
 - b. For turbocharged or supercharged engines, the sequence must be: restrictor, compressor, throttle body, engine.
8. The maximum restrictor diameters at any time during the competition are:
 - a. Gasoline fueled vehicles 20.0 mm
 - b. E85 fueled vehicles 19.0 mm
9. The restrictor must be located to facilitate measurement during Technical Inspection.
10. The circular restricting cross section must NOT be movable or flexible in any way.

11. The restrictor must not be part of the movable portion of a barrel throttle body.
12. Any crankcase or engine lubrication vent lines routed to the intake system must be connected upstream of the intake system restrictor.

The Formula SAE rules lay the baseline requirements for the intake. From there, a team has full creative freedom to design and build anything that can power an engine. The overall goals that this senior design group has established for UVA's 2023 FSAE intake system are as follows:

1. Design an intake manifold that increases the engine's power output by at least 5 horsepower (hp), allowing the vehicle to produce roughly 95 hp.
2. Design an intake manifold that increases the vehicle's fuel efficiency by at least 10%.
3. Decrease the overall weight of the manifold to be less than 75% of the 2022 intake manifold.

The constraints, or limitations, established for this project include:

1. Cost
 - a. \$600 budget from UVA's Senior Design Capstone Course
 - b. \$900 budget from Virginia Motorsports Education
2. Design timeline
 - a. Fall 2022:
 - i. Complete engine simulation for determining runner length
 - ii. Complete design and computational fluid dynamics (CFD) for air flow in restrictor and plenum

- iii. Complete finite element analysis (FEA) for wall thickness optimization
 - b. Spring 2023:
 - i. Finalize research, design, and simulation
 - ii. Manufacture all components
 - iii. Complete testing
- 3. Obtaining an engine simulation software
- 4. CFD modeling of complex airflow within the intake manifold
 - a. How complex will our simulation be based on available data?
 - b. Relating back to Bernoulli and Navier Stokes, how many assumptions do we have to make?
- 5. Minimizing weight
 - a. 75% of 2022 intake manifold
- 6. Are the components manufacturable?
 - a. Can these components either be 3D printed or CNC machined?
- 7. Intake is compliant with FSAE Rules
- 8. Availability of Dyno testing between vehicle completion and FSAE competition

Constraints Screening and Scoring

Table III shows the first 11 rough designs, or concept variants, being scored based on the selection criteria which includes some of the key constraints mentioned above. The main outcomes of completing a concept screening like this include improving manufacturability, reducing lead time, increasing team participation, and having better documentation of the design process (Momot, 2022).

Table III: Concept Screening Results

	Concept Variants										
Selection Criteria	A	B	C	D	E	F	G	H	I	J	K
Simplicity	0	0	0	(-)	(+)	(+)	0	(+)	(+)	(-)	(-)
Reliability	(-)	(-)	(-)	(-)	(+)	(+)	(+)	(+)	(+)	(-)	(-)
Ease of Manufacturing	0	(-)	(-)	(-)	(+)	(-)	(+)	(+)	(-)	(-)	(-)
Cost	(-)	(-)	(-)	(-)	(+)	(+)	0	0	0	0	(-)
Realistic design timeline	(-)	(-)	(-)	(-)	(+)	(+)	(+)	(+)	0	(+)	0
Weight Saving	(-)	(-)	(-)	(-)	(+)	0	(+)	(+)	(-)	(+)	(-)
Engineering Sophistication	(+)	(+)	(+)	(+)	(+)	(+)	(+)	(-)	(-)	0	(+)
FSAE Rules compliant	(+)	(+)	(+)	(+)	(+)	(+)	(+)	(+)	(+)	(+)	(+)
Pluses	2	2	2	2	9	6	6	6	3	3	2
Same	2	1	1	0	0	1	2	1	2	2	1
Minuses	4	5	5	6	0	1	0	1	3	3	5
Net	-2	-3	-3	-4	9	5	6	5	0	0	-3
Rank	7	8	10	11	1	3	2	4	5	6	9
Continue?	no	no	no	no	yes	yes	yes	yes	yes	no	no

This process enabled the team to reduce design possibilities to five variations, E, F, G, H, and I, which can be seen in the figures below. A final scoring can now be done on the remaining five design possibilities. Refer to Table IV.

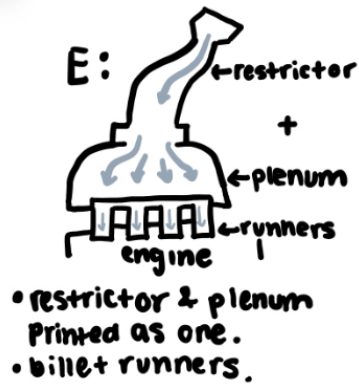


Figure 3. Concept E

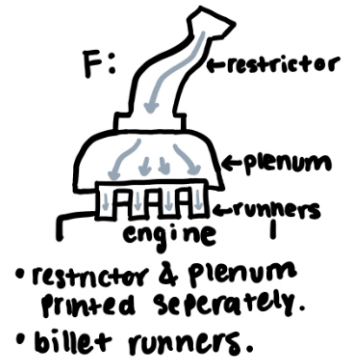


Figure 4. Concept F

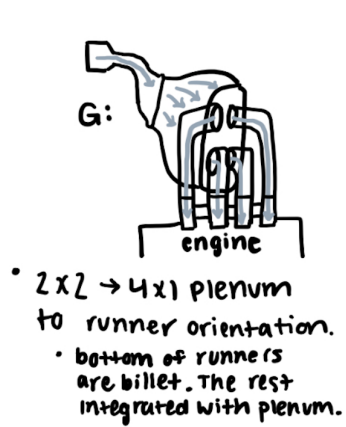


Figure 5. Concept G

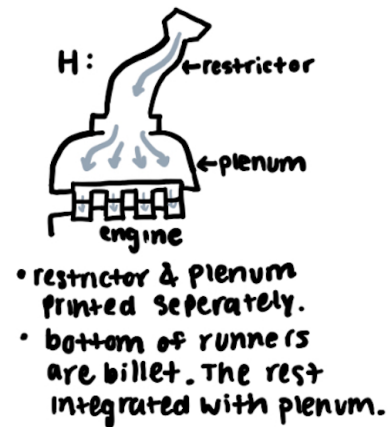


Figure 6. Concept H

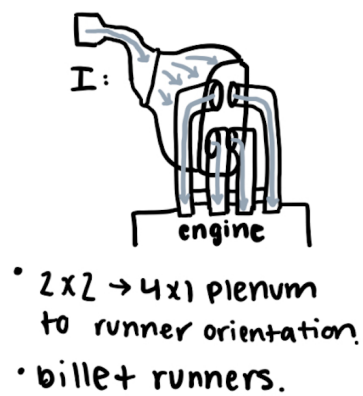


Figure 7. Concept I

Table IV: Scoring Results

	Scoring				
Selection Criteria	E	F	G	H	I
Simplicity	(+)	(+)	0	(+)	(+)
Reliability	(+)	(+)	(+)	(+)	(+)
Ease of Manufacturing	(+)	-	(+)	(+)	-
Cost	(+)	(+)	0	0	0
Realistic design timeline	(+)	(+)	(+)	(+)	0
Actuation Timing/Tuning	0	0	0	0	0
ECU Compatibility	(+)	(+)	(+)	(+)	(+)
Weight Saving	(+)	0	(+)	(+)	-
Engineering Sophistication	(+)	(+)	(+)	-	-
FSAE Rules compliant	(+)	(+)	(+)	(+)	(+)
Pluses	9	7	7	7	4
Same	1	2	3	2	3
Minuses	0	1	0	1	3
Net	9	6	7	6	1
Rank	1	3	2	4	5
Continue?	no	no	yes	no	no

During the Fall 2022 semester, the initial selected design was variant G which consists of a 2x2 plenum to 4x1 runner orientation with the addition of the top half of the runners being integrated with the plenum and the bottom half being made of billet aluminum. After more in depth analysis throughout the fall and winter, it was decided to change the orientation to something more similar to variant H. The original choice, G, was chosen because of the following:

1. Based on prior research, a 2x2 plenum to 4x1 runner orientation will have the most optimal air flow if simulated and designed correctly.
2. The bottom half billet runners will help cool the air prior to entering the engine.

When analyzing various plenum geometries in Ansys Fluent (CFD software), it was found that both the 2x2 to 4x1 runner orientation were able to have very similar flow characteristics. The main point of contention for choosing between these two orientations was to allow for more even distribution of air mass across the four cylinders. From the results generated from ANSYS, it was found that 2x2 orientation has a slightly higher percent difference for mass flow rate across the four cylinders than the 4x1 orientation does. Additionally, choosing the 2x2 orientation would have complicated the design of the runners, making the 4x1 orientation a logical design choice. The team also found that implementing the 2x2 to 4x1 plenum to runner orientation would complicate runner geometry substantially since all runners need to be the same length.

Materials Selection

Prior to starting the design and simulation process, it is important to have materials selected to determine possible manufacturing methods. This can change the design possibilities of a part significantly because of the differences in additive and subtractive manufacturing. For example, for the runners to be made out of aluminum, CNC machining is required which limits parts to not having tight radii. On the other hand, the plenum can be made out of heat resistant plastic like ABS or Nylon so it can be 3D printed, which opens up more organic design possibilities and allows for large hollow features. The following information was used to decide the materials for the intake runners.

Runners (CNC Machined):

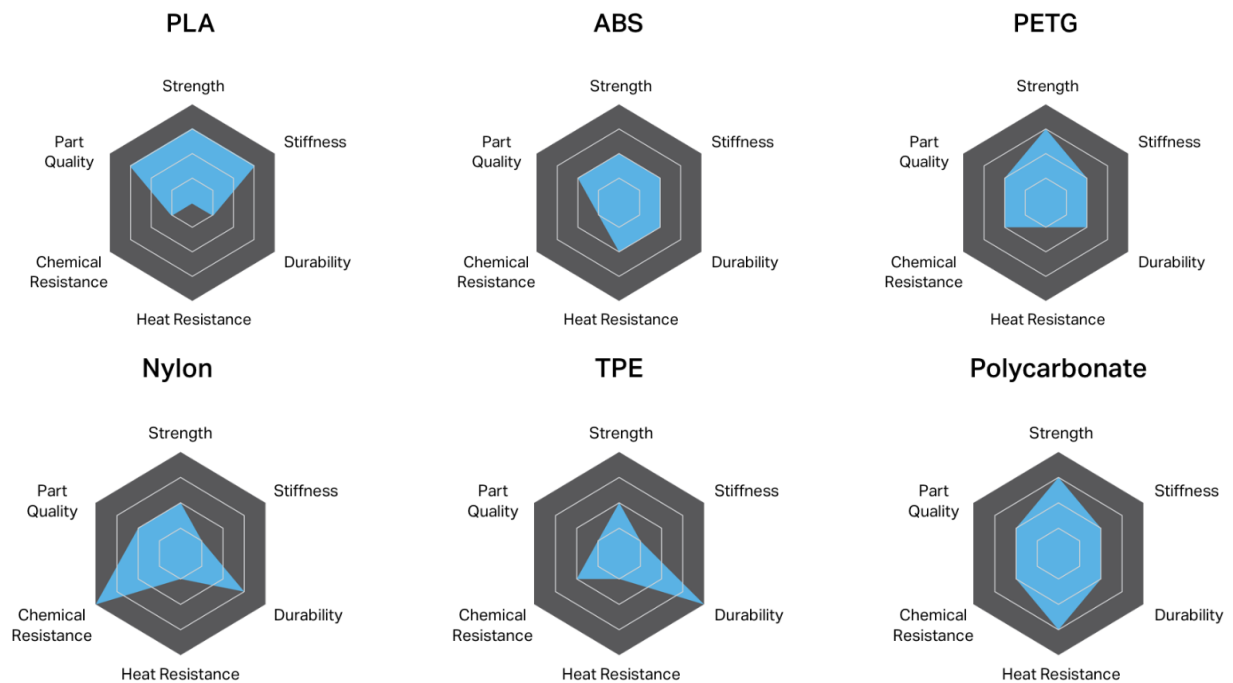
1. Aluminum 6061
 - a. Primarily alloyed with magnesium and silicon.

- b. Good mechanical properties, it is easy to machine, it is weldable, and can be precipitation hardened.
 - c. Excellent corrosion resistance.
 - d. Medium to high strength requirements and has good toughness characteristics.
 - e. Cost effective
 - f. Applications range from aircraft components (aircraft structures, such as wings and fuselages) to automotive parts such as the chassis of the Audi A8.
2. Aluminum 7075:
- a. Considered excellent candidate materials for high-duty structural automotive applications.
 - b. High strength-to-weight ratio, good ductility, and excellent corrosion resistance in most environments.
 - c. Has the highest tensile strength of common aluminum alloys.
3. Aluminum 2024:
- a. Primarily alloyed with copper and magnesium.
 - b. Can be precipitation hardened to strengths comparable to steel
 - c. Susceptible to stress corrosion cracking
4. Aluminum 5052:
- a. The absence of copper allows for better corrosion resistance than Al 6061
 - b. Cannot be heat treated due to the presence of magnesium

It was decided that Aluminum 6061 would be the best option to manufacture the runners this year because it is cost effective and adequate for this application in terms of strength and heat resistance. It is also by far the most commonly used alloy of aluminum, and therefore, the

most readily available by most suppliers. The runners could be integrated with the plenum, and be made completely of plastic, but it was ultimately decided that having roughly 30% of the runners be made of aluminum would help with rigidity and heat isolation. It is also necessary to implement CNC machining to ensure the fine tolerances required for fuel injector port size, location, and angle.

As mentioned previously, the restrictor and plenum will be 3D printed due to their internal geometries. A large range of 3D printed plastics were researched to determine strength, part quality, stiffness, chemical resistance, durability, and heat resistance, but due to the nature of fusion deposition modeling (FDM) 3D printing, most materials were automatically rejected due to their low heat resistance. Figure 8 shows a summary of properties for the initial materials researched.



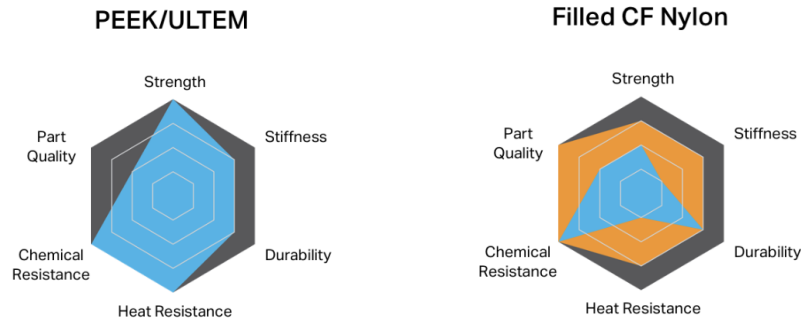


Figure 8. Material property overview of popular FDM 3D printing materials (Markforged, n.d.)

From the materials listed in figure 8, ABS, Polycarbonate, and Filled Carbon Fiber Nylon were selected for further consideration due to their heat resistance. Throughout fall testing of the 2022 Formula SAE car, intake temperature measurements were taken to better understand operating temperatures of that system. Figure 9 shows one set of thermal camera images of intake components roughly 2 minutes after the engine was shut off. These temperatures are much lower than highest operating temperatures but this gave the team an idea of the temperature fluctuation within the intake manifold for material selection and setting CFD parameters.

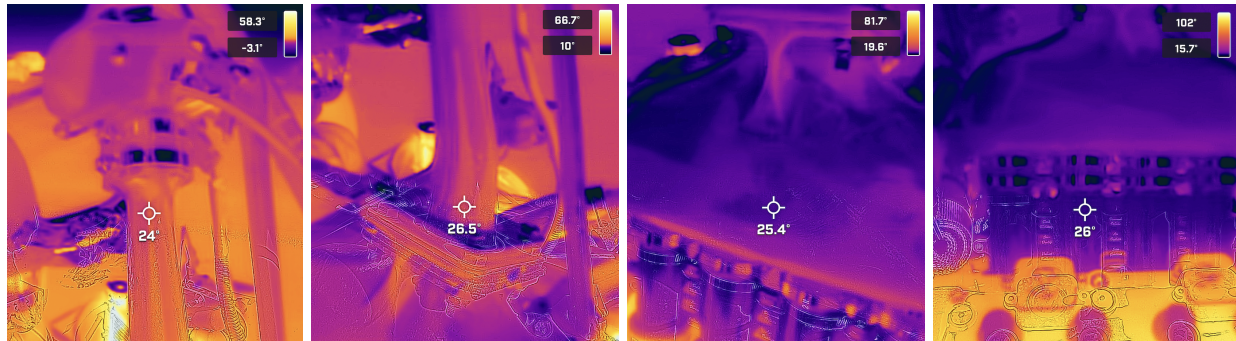


Figure 9. Thermal camera captures (in °C) of intake components

The main considerations for restrictor and plenum materials other than heat resistance were cost and availability. Most free or low cost 3D printing readily available at the university consists solely of PLA and ABS and the bed sizes of most of these printers would not be sufficient to fit the plenum. It was determined that upon request, the Stratasys F170 and F370

printers in the Rapid Prototyping Lab would be sufficient if ABS or Nylon 12 filled with carbon fiber was selected and the Ultimaker S5's in Clemons Library would be sufficient if Polycarbonate was selected. The following information was used to ultimately determine the materials for the restrictor and plenum. All quantitative data was obtained from MatWeb's material properties database and all qualitative data was obtained from Omnexus material selection platform.

1. Acrylonitrile Butadiene Styrene (ABS)

- a. Glass Transition Temperature: 108°C - 109°C
- b. Density: 1.01 - 1.20 g/cc
- c. Tensile stress, yield: 13 - 65 MPa
- d. Modulus of Elasticity:
- e. Good impact resistance, even at low temperatures
- f. Good insulating properties
- g. Good abrasion and strain resistance
- h. High dimensional stability (mechanically strong and stable over time)
- i. Can suffer from stress cracking in the presence of some greases

2. Polycarbonate (PC)

- a. Glass Transition Temperature: 141°C - 150°C
- b. Density: 1.03 - 1.26 g/cc
- c. Tensile stress, yield: 39 - 70 MPa
- d. High mechanical retention up to 140°C
- e. Intrinsically flame retardant
- f. Not brittle

- g. Possesses good abrasion resistance
 - h. Easily attacked by hydrocarbons and bases
 - i. Low fatigue endurance
3. Filled Carbon Fiber (CF) Nylon 12
- a. Glass Transition Temperature: 170°C - 178°C
 - b. Density: 1.11-1.53 g/cc
 - c. Tensile stress, yield: 28 - 103 MPa
 - d. Fibers boost strength, stiffness, and heat resistance significantly
 - e. Excellent surface quality
 - f. Least likely to shrink/warp during printing

It was ultimately decided to use Filled CF Nylon 12 for the restrictor due to the more ductile nature of the material when accounting for the additional vibration experienced by the resistor. It was determined that PC will be used for the plenum due to its low density and higher yield strength in comparison to ABS, which was used for the plenum in 2022.

The final material to be considered is the epoxy resin that will be used to coat the resistor and plenum. Any 3D printed parts contain air bubbles due to the nature of the manufacturing method. The amount and size of these air bubbles can be decreased by decreasing layer height, using a smaller nozzle, increasing shell count, and increasing infill density but they cannot be eliminated completely. Since the restrictor and plenum must be air tight, they need to be coated in a high temperature resistant epoxy resin. There are eight main categories of epoxies which are listed below (*Epoxy Coatings Guide*, n.d.).

1. Amine Epoxy
2. Polyamide Epoxy

3. Amidoamine Epoxy
4. Epoxy Phenolics/Novolacs
5. Siloxane Epoxy
6. Coal Tar Epoxy
7. Water-Based Epoxy
8. Epoxy Esters

Of the eight epoxies listed above, Amine, Polyamide, and Amidoamine were selected for further consideration due to their excellent water/moisture resistance. The selection criteria consisted of high heat resistance (softening temperature > 400 degrees F), water resistant, UV resistant, for use on plastic, sandable, low cost (below \$150 for 1 gallon kit), room temperature curing, and short lead time (less than a month). PRO-SET INF-114 Infusion Epoxy, available through Composite Envisions, was chosen because it met all of the selection criteria, had a competitive price with a short lead time, and will also be used by the carbon fiber team for body panel infusion.

Unfortunately due to printer difficulties with the Ultimaker S5 that would have been used for the plenum printed out of polycarbonate, the team had to default to ABS, printed on one of the Stratasys Fortus printers. Luckily, weight increases were minimal and ABS provided the necessary characteristics needed for a safe operating plenum.

Restrictor Optimization:

The goal of the restrictor is to maximize the venturi effect in the restrictor geometry. The venturi effect is chosen to increase the velocity of the air going into the engine. By the FSAE rules, the restrictor cannot exceed a diameter of 20 mm at the choke point within the geometry (2023 FSAE rules VI). The maximum choke diameter is set to limit the amount of air mass that can go into the engine, thus minimizing the maximum power output. In order to maximize the venturi effect, the pressure loss across the choke point, shown as point two in Figure 10, must be minimized for optimal air mass.

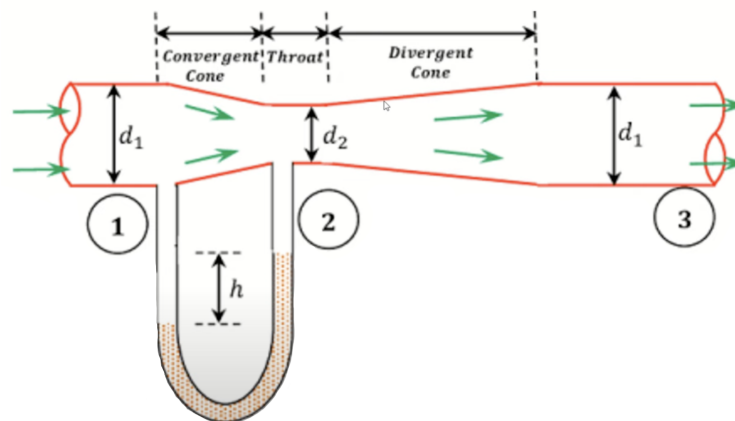


Figure 10. Venturi Effect (citation needed).

The venturi effect can be modeled using Bernoulli's equation for incompressible flow; however, this assumption is only sufficient for Mach numbers below the value of 0.3, as seen in Figure 11. For motorcycle engines, it is typical to see the range of Mach numbers closer to 0.5-0.7, which is in the compressible region of a gas (Winterbone et al., 2001).

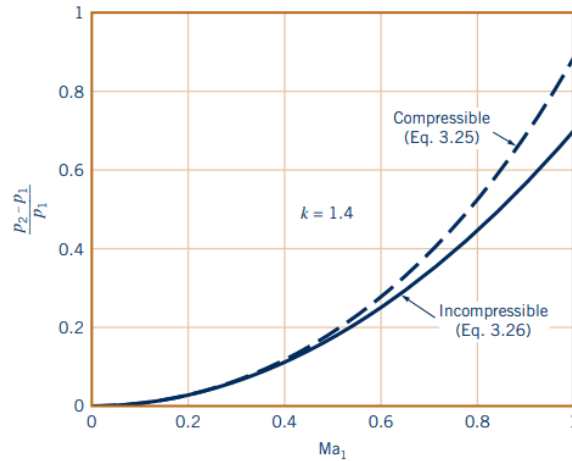


Figure 11. Pressure ratio as a function of Mach number for incompressible and compressible (isentropic) flow (Munson et al., 2013)

For this reason, the Bernoulli interpretation for the venturi effect will be insufficient in providing an accurate metric of the air mass the engine will be receiving. In order to derive a more accurately represented equation, the following assumptions were made (Munson et al., 2013):

- The air that is flowing can be characterized as an Ideal Gas. This allows the ideal gas relations to be used to derive an understanding of how a compressible fluid flows in a simplified manner.
- The fluid is assumed to have isentropic flow, which means there is no change in entropy.
- “Steady-state flow” can also be assumed. This means that the control volume does not change with respect to time, as it is also assumed to be non-accelerating (or inertial).
- One dimensional flow is assumed, which implies uniform flow of the fluid from the inlet and outlet of the control volume, as well as directly perpendicular, as seen in Fig. 8.
- There is constant viscosity assumed for the fluid.

Using isentropic relationships and the thermodynamic equation of state, a mass flow rate equation for compressible flow of an ideal gas can be derived (Hall, 2021). For the purpose of

this restrictor analysis, the optimization is done at the optimal mass flow rate, which for a motorcycle engine is at a Mach number of 1. This is called choked flow at the sonic condition and is interpreted as the velocity of an ideal gas is equal to the speed of sound (Hall, 2021). Assuming a Mach number of 1, the mass flow rate equation for compressible flow of an ideal gas can be simplified to the following equation:

$$m = \frac{APk}{\sqrt{kRT}} \sqrt{\left(\frac{2}{k+1}\right)^{\left(\frac{k+1}{k-1}\right)}} \quad (1)$$

where m is the mass flow rate in kg/s , A is the cross sectional area of the choke point in m^2 , P is the pressure of gas at ambient temperature in Pa , R is the universal gas constant in $\frac{J}{kg \cdot K}$, k is the specific heat ratio, and T is the temperature at ambient conditions in K .

Table V. Values used for calculating maximum mass flow rate

A	$3.14 \times 10^{-4} m^2$
k	1.4
P	102065.75 Pa
R	$286 \frac{J}{kg \cdot K}$
T	297 K

For this restrictor, the maximum mass flow rate through the choked point was calculated to be $0.0752 kg/s$. This was the fixed parameter that was used when optimizing the restrictor geometry using CFD. For the other fixed parameters, the inlet and outlet diameter of the

restrictor is set based on the bore size of the throttle body, which for this restrictor is 42 *mm*. The inlet and outlet diameters remain constant to minimize the velocity losses that are associated with increasing the cross sectional area.

The two most important parameters to iterate through for the restrictor geometry are the converging and diverging angles, which are shown in Figure 8. The convergence angle is altered by changing the location of the choke point along the length of the restrictor. The divergence angle is altered by varying the length of the divergence zone of the restrictor, shown as point 3 in Figure 8. Several iterations of varying these two parameters will be run in the CFD simulation to minimize the pressure loss across the choke point. The final parameter to be changed is the total length of the restrictor. This parameter will not affect the flow characteristics of the venturi effect, but it will have an impact on the throttle response to the engine, which can be optimized using engine simulation software such as Ricardo Wave or GT-Suite. Throttle response is defined as how quickly the car responds to the driver pushing the gas pedal. Cars with little consideration for throttle response will feel significant hesitation when attempting to accelerate by applying pressure to the gas pedal. This makes it extremely important to strike a balance between peak flow and driveability.

The CFD simulation process is comprised of geometry meshing, parameter initialization, and the actual simulation which is governed by the following principles (ANSYS, Inc., 2010):

1. Conservation of mass
2. Conservation of momentum
3. Conservation of energy
4. Conservation of species
5. Effects of body forces

$$\underbrace{\frac{\partial}{\partial t} \int_V \rho \phi dV}_{\text{Unsteady}} + \underbrace{\oint_A \rho \phi \mathbf{V} \cdot d\mathbf{A}}_{\text{Convection}} = \underbrace{\oint_A \Gamma_\phi \nabla \phi \cdot d\mathbf{A}}_{\text{Diffusion}} + \underbrace{\int_V S_\phi dV}_{\text{Generation}} \quad (2)$$

Example equation for complex PDE used in CFD

ANSYS discretizes a domain into a finite number of control volumes, which the user can visualize as a mesh. Equations based on the principles above are then applied to each individual mesh, which explains why creating a more precise mesh results in more accurate results. Figure 12 shows the various mesh types available in Ansys Fluent.

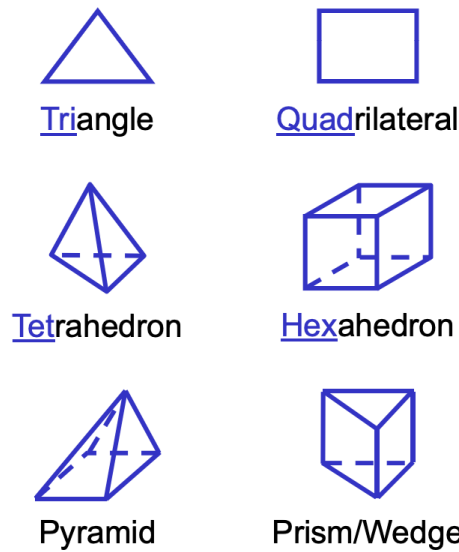


Figure 12. Mesh types in Ansys Fluent

For the restrictor, since it is a flow aligned geometry, a triangular mesh was created because it can provide higher quality solutions with fewer cells than a comparable tri/tet mesh (ANSYS, Inc., 2010). After a mesh is created, solver initialization begins. This consists of defining materials, both solid and liquid, choosing appropriate physical models (turbulence, combustion, multiphase, etc.), prescribing operating conditions and boundary conditions, and setting up solver controls. The following information was used for the CFD simulation:

- a. The inner and outer surfaces of the restrictor were treated as separate bodies to account for airflow going through the restrictor
- b. The size of the triangles in the mesh were automatically optimized in ANSYS
- c. Gravity acts in the Y-direction and is equal to $-9.81 \frac{m}{s^2}$
- d. The inlet port serves as a boundary condition for the mass flow rate of air which is the previously calculated value of 0.0752 kg/s
- e. The outlet port serves as a boundary condition for the air pressure that exits the restrictor
- f. Calculations of CFD results were performed every 20 iterations of the model for 500 iterations. This allowed the results to stabilize which developed a set of average pressure and velocity values which more accurately describes each CFD model.

After completing numerous initial iterations on various diverging and converging angles within the restrictor, optimal angles for maximum velocity flow at the choke point and minimal flow separation were found to be between 4° and 6° . Once the divergent angles were greater than 7° , severe flow separation could be seen in the CFD model which would further restrict the air coming into the engine and is not ideal for driving conditions. An initial restrictor design was created and was iterated through numerous design revisions to continue increasing the velocity. The initial design can be seen in Figure 13 and the final design can be seen in Figure 14. The velocity streamlines calculated on ANSYS can be found in Appendix C.

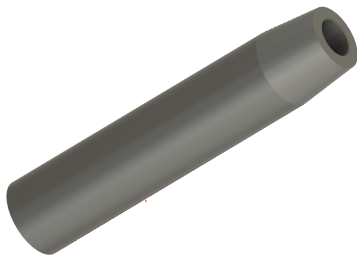


Figure 13. Initial Restrictor Design



Figure 14. Final Restrictor Design

Plenum Optimization:

The goal of the plenum is to provide each cylinder with an even distribution of the air coming from the restrictor. Therefore, the plenum needs to be optimized for smooth air flow, maintaining an even static pressure throughout the chamber, and providing an even amount of air to each of the four cylinders. This is in order to optimize the volumetric efficiency of each piston. ANSYS Fluent was used to analyze the flow and pressure distribution for the various geometries.

Predicting the pressure and velocity distribution for the plenum analytically involves solving several nonlinear partial differential equations. To simplify this approach while also providing accurate results, ANSYS Fluent was utilized to generate the various pressure and velocity profiles for the different geometries, and then post-processed to show streamlines, contours, and vectors, to understand how flow distribution differed with each iteration. In order to conceptually characterize the results and certain trends seen within the graphics, Bernoulli's principle, coupled with general fluid mechanics knowledge, can be used to help hone in on a favorable plenum geometry. In order to apply the simple Bernoulli's equation, the following assumptions need to be made (Munson et al., 2013):

- a. "Steady-state flow" needs to be assumed. This entails that the control volume does not change with respect to time, as it is also assumed to be non-accelerating (or inertial).
- b. Inviscid flow must be considered. This means that the viscous forces are much smaller than the inertial forces within the fluid.
- c. The acceleration due to gravity is maintained constant throughout the application of the problem.
- d. The fluid is incompressible. This means that there is not a sudden change in density within the fluid.

Additionally, Bernoulli's principle must be applied along a constant streamline. After the preceding assumptions are made, the following relationship can be derived:

$$p + \frac{1}{2}\rho V^2 + \gamma z = \text{constant along a streamline} \quad (3)$$

where, p is the static pressure, ρ is the density, V is the velocity of the fluid, γ is the specific weight, and z is the height. The units were not included since this equation is not being used to compute numerical values.

Based on the assumptions described for the restrictor optimization, assumptions b and d are insufficient for this application. The viscosity is considered when configuring the setup for the CFD simulation and assuming incompressible flow would provide inaccurate results based on the Mach numbers that are being seen within the intake system. However, since the actual values for velocity and pressure are not being determined by Eqn. (2), the overall relationship between pressure and flow velocity can be used to understand particular trends seen within the ANSYS results. The trend between incompressible and compressible fluids is similar, as seen in Figure 9, although the numerical solutions deviate by quite a bit once the Mach number exceeds 0.3. For this reason, it is sufficient to use Bernoulli's principle to conceptually interpret the results seen for the various geometries.

There were four iterations for the plenum geometry done. The volume of each was held to be relatively the same across since the primary optimization metric was the flow and pressure distribution. The CAD models for the iterations can be seen in Figures 15 to 18.

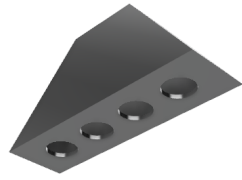


Figure 15. Plenum D0



Figure 16. Plenum D1



Figure 17. Plenum D2



Figure 18. Plenum D3

The initial plenum volume was determined based on the requirements for the engine. The lower limit for the plenum volume is restricted by the displacement of the engine. Since the plenum is acting as an air chamber, the air available needs to be at least the engine displacement. The volume of the plenum can be increased by several factors to allow for more air to be available, which is favorable for horsepower. However, the limiting factor for the plenum volume is the throttle response to the engine, which will have to be considered after optimizing the plenum geometry.

The CFD set-up for the plenum was similar in the beginning as described above for the restrictor. The main difference between the two simulations was the set of boundary conditions in order to ensure that the plenum was being modeled accurately to what can be expected to be seen. The following information was used for the CFD set-up:

- a. The inner and outer surfaces of the plenum were treated as separate bodies to account for airflow going through the plenum

- b. The size of the triangles in the mesh were automatically optimized in ANSYS
- c. Gravity acts in the Y-direction and is equal to $-9.81 \frac{m}{s^2}$
- d. The inlet port serves as a boundary condition for the mass flow rate of air which is the previously calculated value of 0.0752 kg/s . The initial gauge pressure was set to be 102065 Pa which is atmospheric pressure in Michigan.
- e. The outlet pressure served as a boundary condition. Since the engine is pulling a vacuum to pull the air from the plenum down into the runners, the pressure at the outlet had to be set lower than gauge pressure. The outlet pressure was set to read 100000 Pa . This value was roughly based on the Manifold Air Pressure readings seen in the previous year's plenum.
- f. The CFD simulations were performed for 300 iterations, in order to process stable averages of the pressure and flow results across the whole geometry. The run time for each varied, but was roughly around 2-3 minutes per calculation.

The figures for all the post-processed results for the pressure contours, velocity vector profile, and streamline contour are provided within Appendix D. Across the board for all four iterations, some important similarities were seen, which were insightful in ensuring the results were following typical trends based on Bernoulli's principle. As seen in Appendix D, the velocity profile for all four iterations show a sudden increase in velocity at the top of the runners. This is to be expected by Bernoulli's equation, as a sudden decrease in cross-sectional area will result in an increase in velocity and a decrease in static pressure, which can also be seen by the pressure contours provided by ANSYS.

First aspect to consider for the plenum was the smooth air flow. From the ANSYS results shown in Appendix D, Plenum D0, D1, and D2 had fairly turbulent flow on the outer corners of

the plenum. Specifically, D0 was especially rough due to the sharp corners, which causes significant flow losses versus a smoother transition in geometry, as seen in some of the other plenums. The turbulent flow for the first three plenums also causes there to be a lot of flow back up towards the air coming from the restrictor, which further restricts the amount of air that is able to flow into the plenum. This is more easily depicted in the velocity vector results shown in Appendix D, where it can be seen that the flow bounces off the bottom wall and begins to circulate back up towards the restrictor. This is unfavorable, as the function of the plenum is to overcome any losses in mass air flow that is seen in the restrictor. Plenum D3 did not have nearly as much boundary layer separation for the flow. The flow remains fairly laminar throughout, as can be seen in the streamline results from ANSYS in Appendix D. However, there is a pocket of turbulent air at the bottom near the runner farthest away from the entrance point; this turbulent air seems to recirculate and help push more air into the final runner, however, which is beneficial for the function of the plenum.

The second aspect to consider was the static pressure distribution. As seen in the pressure contour maps in Appendix D, all the plenums had relatively even distributions of static pressure excluding Plenum D2. It is extremely important to have even static distribution throughout the plenum, as the flow rate of air going into each cylinder needs to be as equal as possible, and the pressure differential is a major factor in determining how much air will flow into each cylinder.

The final aspect to consider was the mass flow rate of air going into each cylinder. As mentioned before, it is vital that the plenum is able to deliver as even of mass flow into each cylinder as possible, in order to maximize the power output from the engine. As seen in the table below, Plenum D1-D3 were roughly very close to one another with Plenum D0 being the anomaly.

Table VI. Values for mass flow rate into each cylinder

Plenum	Cylinder 1 (kg/s)	Cylinder 2 (kg/s)	Cylinder 3 (kg/s)	Cylinder 4 (kg/s)
D0	0.00128	0.03836	0.03836	0.00136
D1	0.01848	0.02156	0.01698	0.01800
D2	0.01663	0.02120	0.01804	0.01940
D3	0.02270	0.02060	0.01633	0.01533

Based on the above analysis, it was clear that Plenum D1 performed the best in all three of the criteria. Although there is more turbulent flow present, from Table VI, the percent difference in mass flow rate between the four cylinders was the lowest for Plenum D1. The main function of the plenum is to provide as much air as possible, and as even flow between all four cylinders as possible, making the third consideration the most important of the three. Another important consideration with this is the weight that will be on the end of the restrictor. Since the throttle body and air filter hang on the restrictor, it treats the restrictor like a cantilevered beam; hence, further structural analysis to ensure this orientation won't fail under driving conditions is extremely crucial. Given the above analysis and considerations, Plenum D1 was decided as the most optimal and feasible plenum geometry for this system.

Runner Optimization:

The runners pull air from the plenum and send it down to the engine's cylinders. While the plenum is responsible for evenly distributing air to the cylinders, the runners do the actual transporting of air to the engine. There are a few major design considerations for the intake runners which have major impacts on overall peak engine performance as well as general powerband characteristics. The factors considered for this design are runner diameter, runner taper, runner length, and the runner flow characteristics.

These parameters can be used not only to increase the performance of the car but also to improve the driveability and effective powerband for the car. The powerband of the car is a curve which shows the torque produced at given RPMs. These can be obtained theoretically through simulation or empirically through tuning on a chassis dynamometer (dyno). An engine dyno would provide better accuracy for the engine and its components alone but a chassis dyno accounts for external losses like friction, which provides a more accurate model of the car's real world performance for the team. Figure 19 shows the dyno curve for the 2022 FSAE car which uses the same engine that will be used in 2023. The upper curve is horsepower and the lower curve is torque measured in pounds per foot (ft-lbs).

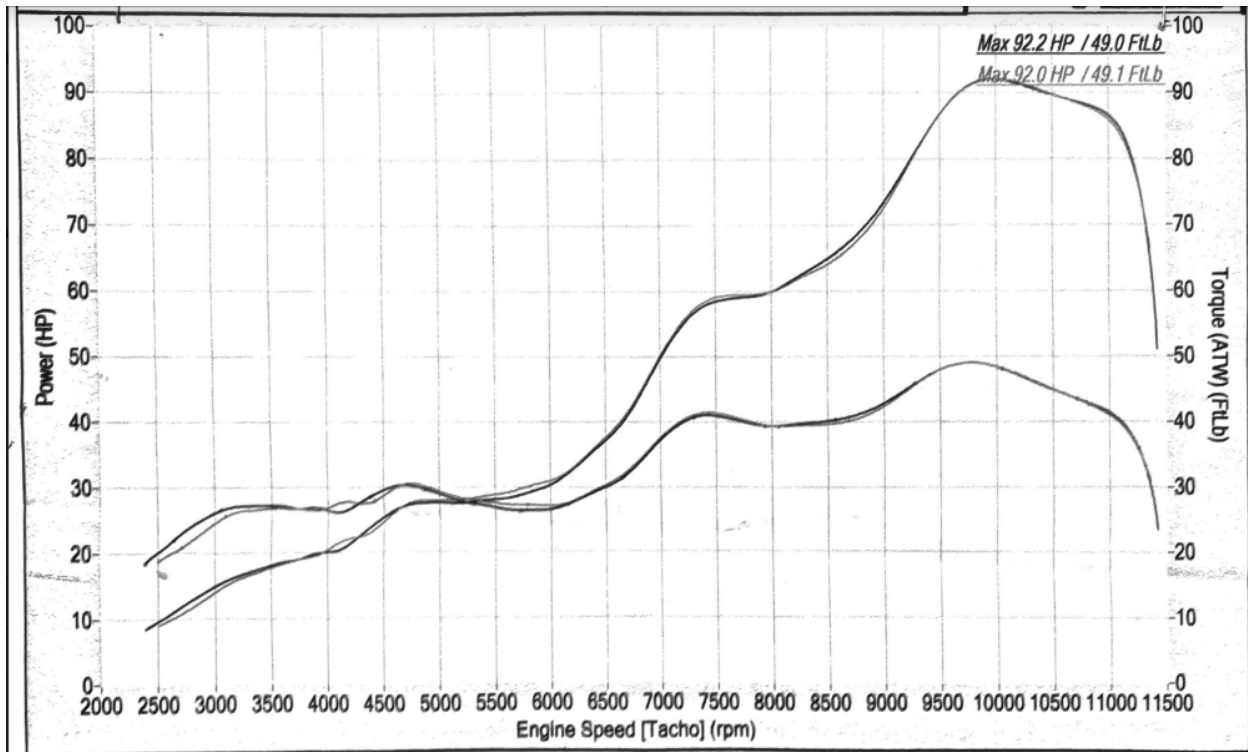


Figure 19. Powerband for 2022 FSAE Car from Chassis Dyno

There are two main styles of tuning for FSAE: One designs for a high powered, but peaky powerband and the other for a smoother powerband which makes good torque throughout a wide range of RPM. A peaky powerband can be good as the ultimate performance of the vehicle is maximized, but it can be difficult for drivers to keep the car in the right operating window in order to actually use this added performance. In an FSAE car, the engine is connected to the wheels with a transmission in between the two. Changing gears allows the driver to adjust the ratio between wheel speed and engine speed. An experienced driver will be able to change gears and keep the car in a tight window where it's making a lot of power. For example, looking at Figure 17, a great driver would be able to keep the car between 9500 RPM and 10500 RPM, where it's making the most power throughout a race. In reality this is very difficult to do while also focusing on racing lines, braking points, and operating conditions of the car. In order to

reduce the need for highly skilled drivers, the engine and intake system will be tuned to have a wider powerband in order to aid in driveability.

The primary goal for the runners this year is to help widen the powerband and make the car more forgiving for drivers across a larger range of RPMs. To help define this, an effective operating window can be established where the car is making a useful amount of torque. For the 2022 car, this window was effectively from 9000 RPM to 11000 RPM, a tight window of only 2000 RPM. This year the goal is to increase this window to around 3 to 4 thousand RPM, which should help drivers keep the engine running to the best of its ability.

Runner length has by far the most impact on the powerband of the car. This is due to resonance within the intake system. The engine has two sets of intake valves which are timed with the engine cycle, opening and closing rapidly. When these valves slam shut, the incoming air stops and it creates a pressure wave which resonates up through the runners and rebounds within the intake system. This rebound can be timed using the speed of sound and the length of the runners such that it rebounds back just as the intake valve is reopening. This effect can be utilized to force more air into the engine, thereby generating more power. The time it takes for this pressure wave to bounce can be calculated using a variety of different methods. To get a starting point, David Vizard's rule of thumb can be used to get a rough estimate of runner length.

$$\text{Runner Length} = (-.0017) * (\text{Designed RPM for Peak Torque}) + 24 \quad (4)$$

Vizard's Equation for Runner length.

This equation was determined empirically, and can be used as a good starting point for further refinement. Plugging in our RPM, the equation yields a runner length of 6.15". To

validate this result, two more equations were used to calculate the runner length. The first of which being the Helmholtz resonator equation.

$$F_p = \frac{162}{k} * c * \sqrt{\frac{A}{LV}} * \sqrt{\frac{R-1}{R+1}} \quad (5)$$

Helmholtz Resonator Equation

This equation uses engine RPM, the speed of sound, cylinder displacement, runner area and compression ratio to solve for runner length. Using this equation the ideal runner length came out to be 6.92 inches. While theoretically this equation would be good for modeling an ideal length for the intake runners in reality it makes far too many assumptions. The most glaring of which are that the entire system is transient, with non constant throttle area, along with rapid temperature and pressure changes which make this equation unreliable for this application. The final equation that will be considered is the Induction Wave Theory Equation.

$$Runner Length = (Effective Valve Closed Duration) * (.5) * (V)/(RPM * Reflective Value) - (D)/2 \quad (6)$$

Induction Wave Theory Equation

This equation uses engine timing in combination with the speed of sound and other minor parameters in order to determine the time it takes for the pressure wave to travel, thus determining runner length. Using this equation the theoretical runner length came out to 6.1 inches, closely matching the empirical solution provided using David Vizard's rule of thumb.

Using these equations the start point for engine simulation will be with a runner length of 6.15 inches.

The runner diameter also has an impact on the performance of the runners. Primarily, it influences the air flow coming into the cylinder. Poorly chosen diameters will result in either restricted flow or low airspeed. The ideal runner diameter increases airspeed which helps fuel atomization and has a small ramming effect in the cylinder, while not reducing the mass flow rate through the runners by a substantial amount. Generally speaking, smaller runner diameters will perform better at lower RPMs where the increase in airspeed helps, and larger diameters better at higher RPMs where the mass flow rate is more impactful. However, runner diameter has substantially less impact on the overall powerband than runner length. To further increase airspeed, typically intake runners will have a small taper in them. Usually this taper is around one degree, and due to the extremely transient nature of the runners, this angle is best determined using engine simulation. To determine runner diameter, David Vizard has an empirically driven equation for determining runner diameter.

$$Diameter = \sqrt{\frac{RPM * Displacement(in^3) * Volumetric Efficiency}{3300}} \quad (7)$$

Vizard's Rule of thumb for runner diameter

Using this a starting diameter of 1.398 inches can be determined for use in engine simulation. Unfortunately, due to the unstable nature of the intake system, simulation leads to the most accurate results when you have multiple parameters to tune all working with each other.

Another aspect to consider is the runner flow characteristics, this is impacted by the other design parameters as described previously, but is also affected by the geometry and quality of the

internal walls of the runners. The runners for this year will be split into two sections, the first being integrated in the 3D printed plenum in order to manufacture the more complex geometry required for the transition from a 2x2 plenum to 4x1 runner configuration. The bottom half of the runners will be machined out of 6061 aluminum to aid in vibrational damping and heat dissipation. It is very important to have smooth surface finishes within both printed and machined runners in order to not disturb the flow through the runners. Similarly, the two halves should have as seamless of a joint between them as possible to further prevent turbulence in the system. To further improve the flow through the runners, the overall shape will also be changed. The port of the engine is shaped like an oval, and this year we will be matching the oval shape with a smooth transition from a circle at the tops of the runners down to the oval shape at the port. The purpose of this is to prevent any disruptions to airflow resulting from the rapid change in diameter and shape where the port meets the runners, turbulence in this area has a significant impact, reducing the ramming effect generated with all the other parameters.

Engine simulation was done preliminarily using Engine Analyzer Pro, which is a 2D engine simulation package where intake parameters and engine specs are entered into the program from which simulations can be run. In the future, a 3D simulation software which incorporates the physical geometry using a CAD model would be more accurate once it becomes available to the team. Engine Analyzer produces both raw data and a basic modeled dyno curve which can be used in order to tune the powerband appropriately. Chain calculations were used to simulate what varying multiple parameters at the same time would do in order to find the best combination of runner length and runner diameter. These are then filtered by average torque, rather than peak horsepower in order to find parameters that flatten out the torque curve. From

these chain calculations a runner diameter of 1.32" and a runner length of 6.25" were determined to be the best solution when looking at the raw numbers and overall smoothness of the curve.

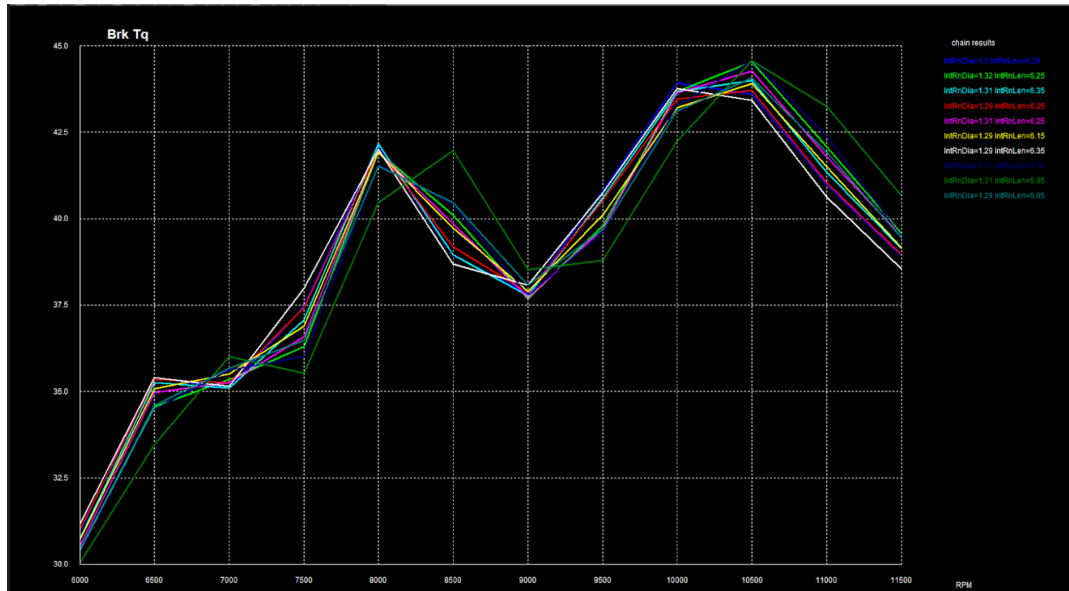


Figure 20. Preliminary Simulation, Runner Diameter and Length variation

From there other smaller parameters can be iterated upon such as runner taper, runner flow specifications, and restrictor flow to see how they impact the torque curve. By starting with the larger adjustments like runner length and diameter, it becomes much easier to follow the impact the smaller fine adjustments make onto the power curve and allows an engineer to more precisely adjust a power curve with the smaller increments caused by minor adjustments to the intake design parameters.

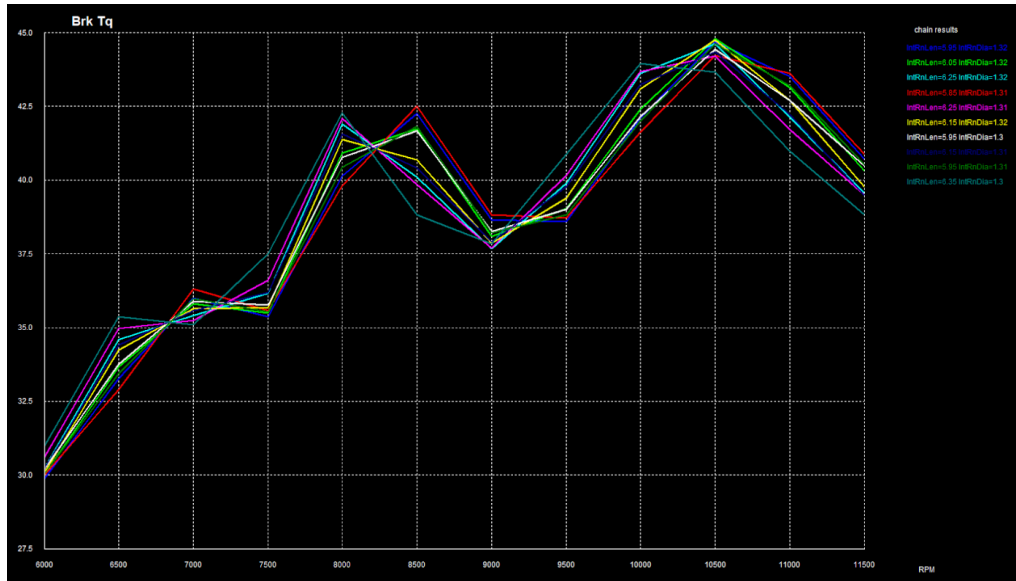


Figure 21. Refined Runner Length and Runner diameter simulation

Engine RPM	6000	6500	7000	7500	8000	8500	9000	9500	10000	10500	11000	11500
Chain # 4 (3.6" Hg Idle Vac, 36.58 cid)												
IntRnLen=6.15 Tq	30.19	34.24	35.60	35.80	41.44	40.79	37.80	39.34	43.20	44.76	42.80	39.66
HP	34.49	42.37	47.45	51.12	63.12	66.02	64.78	71.16	82.25	89.48	89.63	86.85
Chain # 5 (3.6" Hg Idle Vac, 36.58 cid)												
IntRnLen=6.25 Tq	30.34	34.49	35.35	36.19	41.79	40.04	37.71	39.92	43.64	44.54	42.07	39.50
HP	34.66	42.69	47.12	51.68	63.66	64.80	64.62	72.21	83.10	89.05	88.12	86.50
Chain # 2 (3.6" Hg Idle Vac, 36.58 cid)												
IntRnLen=5.95 Tq	29.86	33.24	36.05	35.36	40.19	42.28	38.59	38.67	42.09	44.55	43.44	40.76
HP	34.11	41.14	48.04	50.49	61.23	68.43	66.13	69.95	80.15	89.07	90.97	89.25
Chain # 3 (3.6" Hg Idle Vac, 36.58 cid)												
IntRnLen=6.05 Tq	30.05	33.59	35.77	35.48	40.76	41.43	38.18	38.91	42.49	44.67	43.07	40.39
HP	34.33	41.58	47.67	50.67	62.09	67.05	65.42	70.38	80.91	89.31	90.20	88.44
Chain # 6 (3.5" Hg Idle Vac, 36.58 cid)												
IntRnLen=6.35 Tq	30.53	34.98	34.97	36.54	41.65	39.02	37.63	39.97	43.51	43.94	41.38	38.79
HP	34.87	43.30	46.61	52.18	63.44	63.16	64.48	72.29	82.85	87.84	86.67	84.93
Chain # 1 (3.6" Hg Idle Vac, 36.58 cid)												
IntRnLen=5.85 Tq	29.85	32.99	35.51	35.07	39.87	41.40	38.44	38.52	41.58	43.83	43.07	40.43
HP	34.11	40.83	47.33	50.08	60.74	67.00	65.88	69.67	79.18	87.63	90.20	88.53

Figure 22. Final Torque and Horsepower numbers generated by Engine Analyzer Pro

The final aspect to consider for the intake runners is the injector angle and location. The fuel injectors control the amount of fuel the engine receives and what time within the engine cycle that it receives the fuel. An injector is mounted on the runners and sprays fuel into the airstream at tuned intervals. Fuel atomization is essentially how well the fuel and air are mixed together. The better the air and fuel are mixed, the cleaner and more powerful the combustion process will be. Since the competition gives out points for efficiency, this is an important factor

to consider. In order to achieve best atomization, the angle that the injectors are mounted at would be directly within the airstream however this would significantly impact the airflow, and as such the injector is mounted slightly outside the airstream with as steep an angle as possible with manufacturing constraints. For this year, the port angle will be 15 degrees, which was found to be the steepest orientation possible when considering tool clearance during CNC milling.

Another design optimization to be made is the height of the injectors. In order to best atomize the fuel, the fuel should be sprayed when the intake valve is closed and the mixture should bounce off the back of the valve being “swirled” using the motion of the intake valve opening. In order to generate this effect, the height of the injectors from the back of the valve must be adjusted in conjunction with the injector angle. This height can be measured empirically once the preliminary design of the runners is done and further validated using a 3D engine simulator.

Connections:

To accommodate for the restrictor and plenum being printed separately, proper connections need to be made to ensure an airtight seal. This can be accomplished in a variety of ways including, but not limited to, bolted connections, snap fits, riveting, adhesives, and ultrasonic welding. Snap fits and riveting would not provide the strength required to obtain an airtight seal when considering the vibration the intake encounters. Ultrasonic welding with an epoxy resin coating would work very well but the technology is not readily available. Using an adhesive to seal the two together would also be a good sealing method, but if there were issues with the bonding, both the plenum and restrictor would need to be printed again which is unfavorable due to the limited materials and manufacturing timeline. It was ultimately decided to use properly spaced bolts, with a gasket between the two materials, because with proper gasket selection, bolt hole spacing and sizing, and torque specking, the two materials can easily be sealed air tight.







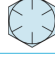

To determine the proper bolts to be used, the following factors must be considered (UC Components Inc., 2021):

1. Load
 - a. Proof load: the limit of the elastic range of the bolt.
 - b. Yield strength: the load at which the fastener will become permanently deformed.
 - c. Tensile (ultimate) strength: the load that will break the fastener.
2. Resistance properties
 - a. Corrosion wears metal down due to the material's interaction with chemicals in the surrounding environment.
3. Temperature

- a. Connections must be able to withstand operating temperatures. For example, some materials can become brittle in extreme cold and lose their ductility.

To be in compliance with the 2023 FSAE rules, all bolts used in the intake manifold must be made of at least SAE Grade 5 steel (2023 FSAE rules VI, n.d.) and all nuts must have positive locking mechanisms such as nyloc or distortion. While aluminum bolts might have been sufficient and saved a small amount of weight, steel bolts provide excellent strength, low corrosion resistance, and can withstand high temperatures (UC Components Inc., 2021). They are also the most commonly used material for bolts and are low in cost. Table VII shows relevant properties for SAE Grade steel bolts that will be used for determining the grade selection.

Table VII: SAE Specifications for Steel Bolts (Shigleys, 2007)

SAE Grade No.	Size Range Inclusive, in	Minimum Proof Strength,* kpsi	Minimum Tensile Strength,* kpsi	Minimum Yield Strength,* kpsi	Material	Head Marking
1	$\frac{1}{4}$ – $1\frac{1}{2}$	33	60	36	Low or medium carbon	
2	$\frac{1}{4}$ – $\frac{3}{4}$ $\frac{7}{8}$ – $1\frac{1}{2}$	55 33	74 60	57 36	Low or medium carbon	
4	$\frac{1}{4}$ – $1\frac{1}{2}$	65	115	100	Medium carbon, cold-drawn	
5	$\frac{1}{4}$ –1 $1\frac{1}{8}$ – $1\frac{1}{2}$	85 74	120 105	92 81	Medium carbon, Q&T	
5.2	$\frac{1}{4}$ –1	85	120	92	Low-carbon martensite, Q&T	
7	$\frac{1}{4}$ – $1\frac{1}{2}$	105	133	115	Medium-carbon alloy, Q&T	
8	$\frac{1}{4}$ – $1\frac{1}{2}$	120	150	130	Medium-carbon alloy, Q&T	
8.2	$\frac{1}{4}$ –1	120	150	130	Low-carbon martensite, Q&T	

*Minimum strengths are strengths exceeded by 99 percent of fasteners.

With bolt type and material selected, the last consideration is properly sizing them to ensure adequate clamping force in the joint. This is important for ensuring that there is no shear, bending, or excessive dynamic loading. Oversizing bolt diameter to ensure adequate clamping force is a misconception that many students have and not always correct because it can often

result in a joint with low clamp load, high risk for failure due to fatigue, increased cost, and difficulty with proper tightening. The bolts securing the restrictor and plenum experience a variety of loads that can be simulated in a multitude of ways, but due to the limited variables available for complex computations, a simple vibrational analysis and incorporating a slightly higher safety factor will suffice. If the necessary variables were available, an in depth clamping force could be calculated when considering internal plenum pressure, pressure drop in the restrictor, force on the restrictor due to air resistance, and engine vibration. This would provide enough information to do an in depth optimization of bolt diameter, length, and grade.

Based on the pressure forces experienced within the plenum, which is around 8000 Pa, and the vibration that the intake members experience due to the engine, which varies substantially based on RPM, 4 Grade 8 Steel, 3/8"-16 Thread Size, 1" Long would be adequate, but due to some minor sealing issues that occurred in 2022, 6 Grade 8 Steel, 10 mm-24 Thread Size, 3/4" Long would provide a better seal. Not only does it provide a better seal, it will also help with more even pressure distribution at the connection.

The use of a gasket is a necessity in this application, as the solid surface of the restrictor and the top of the plenum are unlikely to sit precisely flush with one another. This can be caused by differing tolerances when printing, a slightly uneven printing bed, and a variety of other external factors that cannot be feasibly controlled within the design. The uneven mating of two surfaces leads to potential air pockets for the fluid to escape through, which would negatively affect the overall functionality of the air intake system. In order to maintain a favorable pressure differential in the system, eliminating all routes for leakage is crucial. A gasket can be placed and compressed between the two surfaces to eliminate potential air pockets.

In order to select a suitable gasket for this application, a number of considerations must be adhered to (Taraborelli, 2022):

1. Load
 - a. The force exerted by the bolts and the two mating surfaces on the gasket will impose a particular pressure distribution. Gaskets have an optimal compression range to allow for proper sealing; however, if the pressure exceeds the maximum rated pressure, the gasket is prone to wear and will be unusable if unloaded.
2. Temperature
 - a. The gasket material must be able to withstand the operating temperature of the system to avoid failure due to corrosion or permanent deformation.
3. Corrosion Resistance
 - a. Gasket materials must be rated to sustain in the presence of certain chemicals and fluids, such as gasoline and oil.

Within these considerations, a variety of different gasket types are available and listed below (Taraborelli, 2022):

- a. Metallic gaskets
- b. Non-Metallic/Soft gaskets
- c. Semi-Metallic/Composite gaskets

Metallic gaskets are typically used in high pressure applications, with pressure ratings ranging up to 20,000 psi (Taraborelli, 2022). For the air-intake system, the entire system is pulled in a vacuum; therefore, metallic gaskets are not a common material for this application.

Additionally, since the need for a gasket in this application is for sealing uneven surfaces, the gasket material chosen must have some compressibility and ability to flex to seal any air-pockets

within the two surfaces. Softer gaskets are also the easiest to manufacture into the shape of the bulkhead, as well as cost effective. For this reason, and to simplify the analysis, only gaskets of materials from b were considered.

Non-Metallic/Soft Gaskets typically consist of Compressed Non-Asbestos Fiber (CNAF), Graphite, Polytetrafluoroethylene (PTFE), Rubber, and Teflon (Taraborelli, 2022). Within each of these denominations, there are several different grades and variations which each are individually rated for various temperatures, various operating pressures, and are resistant to different chemicals. Within these subcategories, rubber is the most readily available and has a variety of types which can be evaluated for this application. To avoid an exhaustive analysis, rubber was the gasket material chosen to consider for this application, as it is commonly used in sealing mating surfaces for systems involving oil and gasoline (McMaster-Carr, n.d.). As seen in Figure 23, there are several types of rubber gasket material to choose from and each is resistant to different chemicals.

	Minimum Temp., °F	Maximum Temp., °F	Acetic Acids	Animal/Veg-etable Oils	Detergents	Gasoline	Grease	Hydraulic Oils	Isopropyl Alcohol	Salt Water	Steam	Synthetic Lubricants	Water
Multipurpose													
Neoprene	0°	200°			•				•	•			•
High Temperature													
Silicone	-60°	400°	•		•				•	•			•
Oil Resistant													
Buna-N	-20°	170°		•	•	•	•	•	•	•			•
Buna-N/Vinyl	-20°	200°		•	•	•	•	•	•	•			•
Chemical Resistant													
Viton® Fluoroelastomer	0°	400°		•	•	•	•	•	•	•	•	•	•
Aflas	40°	400°			•	•		•	•	•	•	•	•
Fluorosilicone	-65°	450°		•		•	•	•	•	•			•
Kalrez	0°	525°	•	•	•	•		•	•	•	•		•
Abrasion Resistant													
Polyurethane	-10°	200°		•		•	•						•
Natural Gum	-20°	140°			•				•	•			•
SBR	-20°	170°								•			•
Weather-Resistant													
EPDM	-40°	225°	•		•				•	•	•		•
Butyl	-40°	225°	•		•				•	•	•		•
Santoprene	-50°	250°	•				•			•			•

Figure 23. Rubber materials and their resistance characteristics (McMaster-Carr, n.d.)

Based on Figure 23, it is important to choose a gasket material that can withstand gasoline and oil, since both are circulated through the engine and the essence of both can be seen in the intake, although unlikely, so the gasket must be able to withstand both. Based on this criterion, the two materials to dive deeper into are Buna-N and Buna-N/Vinyl. Buna-N is also known as nitrile, and is known for its resistance to oil, gasoline, and grease (McMaster-Carr, n.d.). One more important factor to consider for gasket material is the relative hardness or softness. This can be numerically calibrated on the Durometer Hardness Scale (McMaster-Carr, n.d.). There are three different scales that they are determined off of: Shore A, Shore B, and Shore OO. The relation between the three scales can be seen in Figure 24 below.

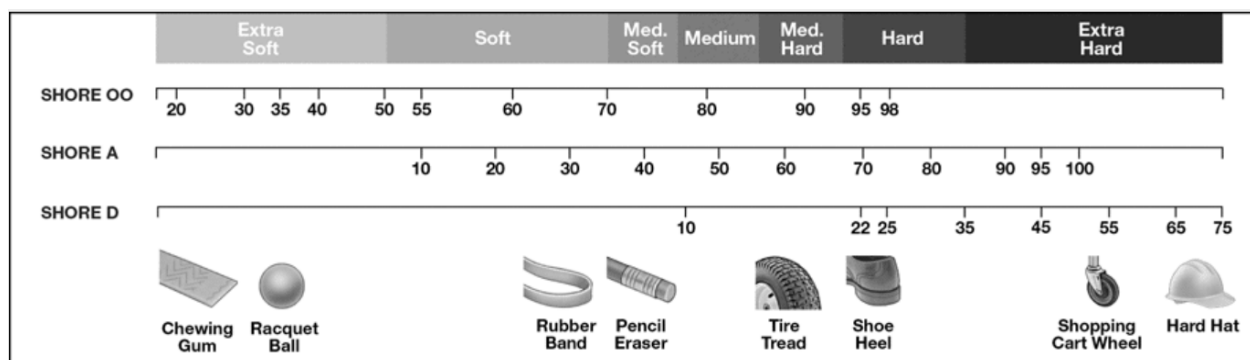


Figure 24. Durometer Hardness Scale (McMaster-Carr, n.d.)

Below are some important characteristics about Buna-N:

- Operating temperature: -20°F to 170°F
- Tensile Strength: 800 psi
- Durometer Hardness Number: 40A (Medium Soft), 50A (Medium)

Below are the important characteristics about Vinyl:

- Operating temperature: -20°F to 220°F
- Tensile Strength: 1,500 psi

c. Durometer Hardness Number: 70A Hard

From a rudimentary comparison between the typical applications used for both, Buna-N is more commonly used in automotive applications involving fuel and oil. Vinyl is typically used in the food industry, and is known for its resistance to animal and vegetable oils. Although the tensile strength and operating temperature range are larger for Vinyl, since the application of it is not typical in automotive, it was determined that it may not be sufficient for this intake system. Additionally, it is relatively hard, and has the same hardness as a shoe heel, which means it would not have as much compressive strength to fill in air pockets. Since the main purpose of the gasket is to mesh two uneven surfaces of the restrictor and plenum together, having a softer gasket will allow it to compress and shape shift to even out the surfaces. Softer gaskets are also seen in more applications involving vacuum sealing, which is the case of this plenum (*Gasket Pressure Guide*, n.d.). For these reasons, Buna-N was chosen as the gasket material.

Structural Analysis:

It is difficult to quantify the effects of vibrational loads, as they are random in nature and often have high uncertainties when attempting to predict them. Finite element analysis, used in conjunction with structural analysis, allows us to analyze the vibrational forces exerted on the intake system. For this project, Solidworks software was used to conduct random vibrational analysis tests on the assembly of the intake system. This analysis was done in order to minimize part thickness, and in turn the weight of the system, as well as determine the strength and reliability of each connection between parts and the engine, helping to insure its longevity. The output quantities that are used in random vibration analysis to understand the behavior of the structure are: stress, strain, and directional displacements. By knowing the concentrations of

stress and strain within the system at different natural frequencies and constraining specific areas to allow no displacement, the likelihood of part failure can be quantified. In order to find these output quantities, data from the current system must be input. The vibrational loads were applied from the top of the runners and the bottom are fixed to the engine block. The mounting locations of the intake manifold, and bottom faces of the runners, were constrained to allow zero displacement. The acceleration load levels for the range of the random vibration are determined with respect to engine speed (RPM). The frequency range used in these tests was from 0 Hz to 333 Hz, based on an RPM range of 0 RPM to 20,000 RPM. This allows the test to be within a large factor of safety as the engine operates at a max of approximately 11,000 RPM. The material and geometric properties of the intake are used by Solidworks in this computation as well.

Preliminary tests were conducted on the individual components of the system to gain an understanding of what natural frequencies each part resonates at. The resonance of a part is where at a specific frequency, the vibration becomes amplified causing the part to experience the most stress. It occurs when a vibration is transmitted to another object whose natural frequency is similar to that of the source. The results from these tests revealed that the parts are not within a vibrational range to create resonance.

Following these initial tests an analysis of the entire intake assembly needed to be conducted to ensure it could sustain the vibrational loads from the engine. First, the natural frequencies of the assembly itself were found and are depicted in the figure below.

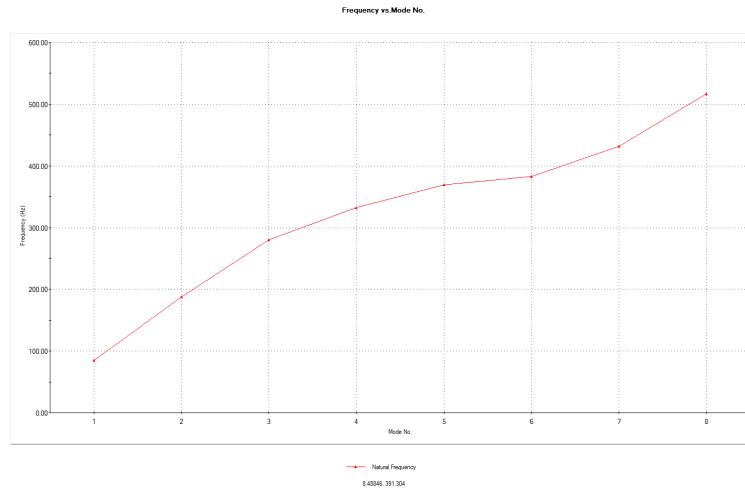


Figure 25. Natural Frequencies of Intake Assembly

Having these frequency values is crucial to determining the parts failure. Now having the natural frequencies of each part and the assembly itself we can begin to test our intake. Each natural frequency was noted and a random vibrational analysis was conducted on the assembly using a three sigma factor. As random vibration has a statistical input, the output is also statistically in nature and follows a Gaussian distribution. Using a three sigma factor ensures that we are covering 99.7% of probabilistic outcomes.

For a random vibrational analysis you want your results to be a plot of power as a function of frequency to determine which frequencies your part experiences the most energy at. Acceleration of the part during vibration can be used to create a response power spectral density (PSD) graph. PSD graphs allow you to see the expected frequency of the system, in other words what frequency leads to the most power. Our tests show an expected frequency of 509.76 Hertz, producing a resultant total power of $206 \frac{g^2}{Hz}$. The resultant PSD graph and stress concentrations of the assembly subject to random vibration can be seen in the following figures.

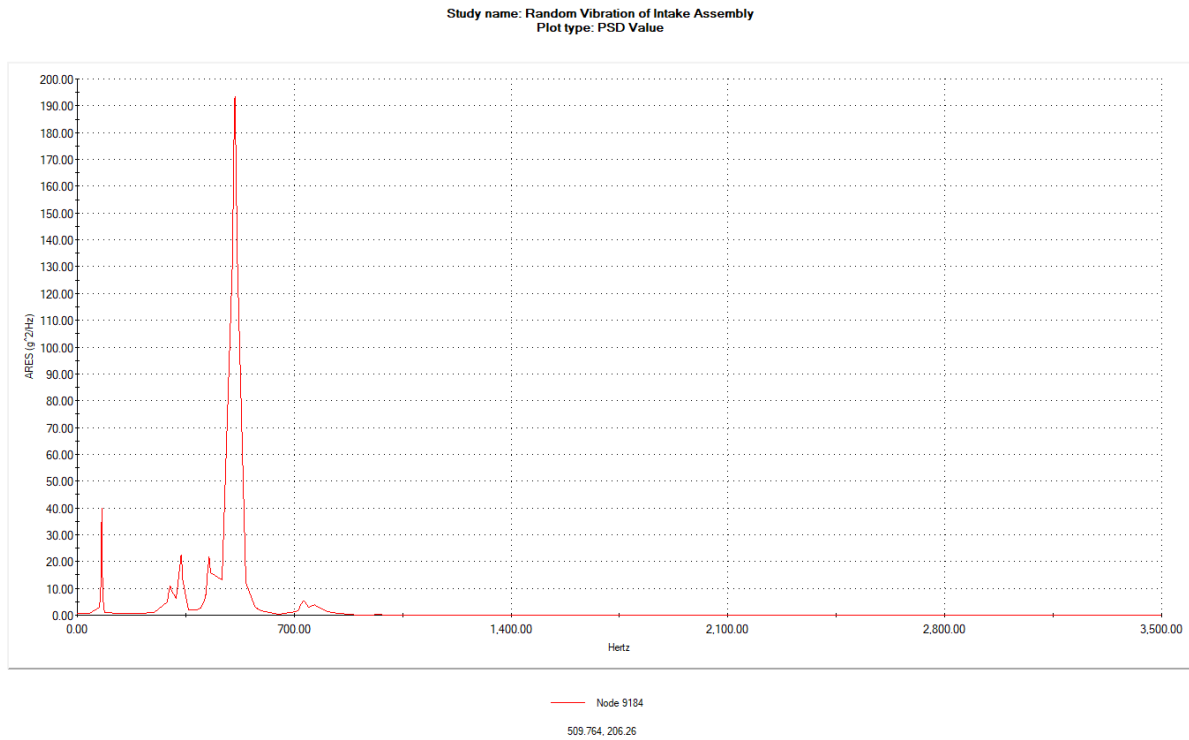


Figure 25. Resultant PSD of Intake Assembly Subjected to Random Vibration

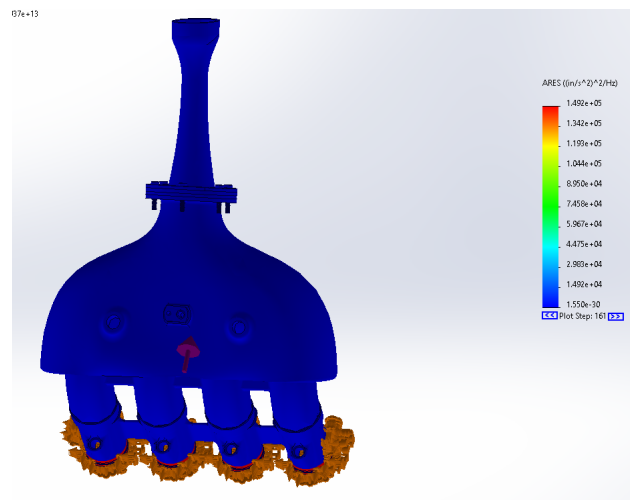


Figure 26. Stress Distributions of Assembly Subjected to 11,000 RPM

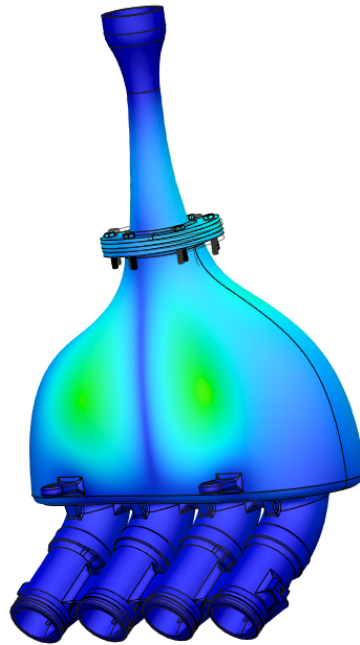


Figure 27. Stress Distributions of Assembly at expected frequency

The resultant power of the expected frequency is enough to deform our part slightly and leads to large concentrations of stress as seen in Fig. 27. Permanent deformation and damage to the assembly will only occur if it is kept at the expected frequency for prolonged periods of time. However, a frequency of 509 Hertz is roughly 30,500 RPM. This is far beyond the RPM range that our engine will operate in. Therefore, the team concluded that our part is able to withstand the vibrational loads that the engine will produce, and not in any danger of failing. As seen in figure 26, the stress the intake assembly experiences at a normal operating frequency of 11,000 RPM is very minimal.

The figures and results shown in this report are of the last iteration of vibrational testing. Three other analyses were conducted on the intake assembly with varied part thickness. By increasing or decreasing the thickness of the assembly the resultant expected frequency would


shift. The final thickness of each part was chosen because it led to an expected frequency that occurred outside of the engine's operating range. These analyses were also conducted without taking the epoxy coating of restrictor support into account, leaving us with an added source of protection from vibrational loading. Future work and analysis can be conducted to reduce the thickness of the intake even more. ANSYS vibration analysis software would allow us to input more specifications, helping us to test with higher accuracy. If done earlier in the design phase different materials could have also been tested to find a material that can withstand higher vibrational loads and in turn reduce the weight.

Manufacturing Phase - 3D Printing

The fall semester of work for this senior design project consisted primarily of research, design, and simulation, all of which brought further insight into the best restrictor, plenum, and runner geometries. While there was extensive simulation done on various restrictor and plenum geometries, the most optimized of each would not be compliant with each other and therefore more plenum and restrictor models were designed and flow tested. It was decided to do more analysis on plenum D1 because it had the most favorable packaging allowances and provided the best restrictor geometry as well. Throughout the winter, the team finalized the intake assembly and began design reviews and finalizing manufacturing methods (print orientation for restrictor and plenum, CAM for runners, etc). Design reviews consisted of the entire team reading through all FSAE rules and checking for compliance and inspecting all connection geometries to ensure proper fitment.

While the restrictor and plenum designs were finalized at this point, both will be 3D printed and require additional research to optimize slice settings and print orientation. The first thing that was determined was how to obtain precise holes for bolts since they cannot be too tight or loose. It was found that holes built using FDM, smaller than 1 in. (25 mm), are typically slightly undersized. When tighter tolerances are required, these holes can be drilled and reamed to ensure accuracy. This led to more in depth research on print settings. Some key pieces of information for the prints are as follows:

1. Restrictor:
 - a. Printer: Stratasys Fortus 380 with 0.6 mm diameter nozzle
 - b. Material: Nylon 12 CF
 - c. Specific tolerances for this printer and material: ± 0.008 in.
 - d. Build volume: 14x12x12"



	FDM Nylon 6	FDM Nylon 12	FDM Nylon 12CF	PC	PC-ISO
	Stratasys F900	Fortus 360mc	Fortus 450mc	Fortus 360mc	Fortus 380mc
System Availability		Fortus 380mc	Stratasys F900	Fortus 380mc	Fortus 400mc
		Fortus 400mc		Fortus 400mc	Fortus 450mc
		Fortus 450mc		Fortus 450mc	Stratasys F900
		Stratasys F900		Stratasys F900	
Layer Thickness	0.013 inch (0.330 mm)	0.013 inch (0.330 mm)	.010 inch (0.254 mm)	0.013 inch (0.330 mm)	0.013 inch (0.330 mm)
	0.010 inch (0.254 mm)	0.010 inch (0.254 mm)		0.010 inch (0.254 mm)	0.010 inch (0.254 mm)
		0.007 inch (0.178 mm)		0.007 inch (0.178 mm)	0.007 inch (0.178 mm)
				0.005 inch (0.127 mm) ^{1,5}	
Support Structure	Soluble	Soluble	Soluble	Breakaway, Soluble	Soluble
Available Colors	■ Black	■ Black	■ Black	□ White	□ White ■ Translucent Natural
Tensile Strength (Ultimate) ²	XZ: 9,800 psi (67.6 MPa)	XZ: 6,650 psi (46 MPa)	XZ: 10,960 psi (75.6 MPa)	XZ: 8,300 psi (57 MPa)	XZ: 8,300 psi (57 MPa)
	ZX: 5,300 psi (36.5 MPa)	ZX: 5,600 psi (38.5 MPa)	ZX: 4,990 psi (34.4 MPa)	ZX: 6,100 psi (42 MPa)	
Tensile Elongation ²	XZ: 38%	XZ: 30%	XZ: 1.9%	XZ: 4.8%	XZ: 4%
	ZX: 3.2%	ZX: 5%	ZX: 1.2%	ZX: 2.5%	
Flexural Stress	XZ: 14,100 psi (97.2 MPa)	XZ: 9,700 psi (67 MPa)	XZ: 20,660 psi (142 MPa)	XZ: 13,000 psi (89 MPa)	XZ: 13,100 psi (90 MPa)
	ZX: 11,900 psi (82 MPa)	ZX: 8,800 psi (61 MPa)	ZX: 8,430 psi (58.1 MPa)	ZX: 9,900 psi (68 MPa)	
IZOD Impact, notched	XZ: 2.0 ft-lb/in (106 J/m)	XZ: 2.5 ft-lb/in (135 J/m)	XZ: 1.6 ft-lb/in (85 J/m)	XZ: 1.4 ft-lb/in (73 J/m)	XZ: 1.6 ft-lb/in (86 J/m)
	ZX: 0.8 ft-lb/in (43 J/m)	ZX: 1 ft-lb/in (53 J/m)	ZX: 0.4 ft-lb/in (21.4 J/m)	ZX: 0.5 ft-lb/in (28 J/m)	
Heat Deflection at 264 psi	93 °C (199 °F)	82 °C ⁶ (180 °F) ⁶	143 °C (289 °F)	127 °C (261 °F)	127 °C (260 °F)
Unique Properties	Very high strength and toughness combined	Fatigue-resistant, high elongation at break	Highest flexural strength of any FDM material	Strong (tension)	ISO 10993 USP Class VI ⁴

¹ 0.005 inch (0.127 mm) layer thickness not available for Stratasys F900.

² See individual material spec sheets for testing details.

³ 0.013 inch (0.330 mm) layer thickness for PPSF not available on Stratasys F900.

⁴ It is the responsibility of the finished device manufacturer to determine the suitability of all the component parts and materials used in their finished products.

⁵ PC can attain 0.005 inch (0.127mm) layer thickness when used with SR-100 soluble support.

⁶ Annealed.

⁷ Actual surface resistance may range from 109 to 106 ohms, depending upon geometry, build style and finishing techniques.

⁸ Available only on the Stratasys F123 Series.

⁹ Available only on the Stratasys F370.

¹⁰ Available on Fortus 400mc and Stratasys F900.

¹¹ Available on the Stratasys F900 only.

^{*} Available on Fortus Classic only.

^{**} Mechanical properties are measured on the Fortus systems and may vary with other printers.

Figure 26. Stratasys Fortus 380mc Printer Information

2. Plenum:

- Printer: Ultimaker S5 with 0.4 mm diameter nozzle
- Material: Polycarbonate
- XYZ resolution (tolerance): 6.9, 6.9, 2.5 micron
- Build volume: 13x9.4x11.8”

Ultimaker S5 specifications

Printer and printing properties	Technology	Fused filament fabrication (FFF)
	Print head	Dual extrusion print head with a unique auto-nozzle lifting system and swappable print cores
	Build volume (XYZ)	330 x 240 x 300 mm (13 x 9.4 x 11.8 in)
	Layer resolution	0.25 mm nozzle: 150 - 60 micron 0.4 mm nozzle: 200 - 20 micron 0.6 mm nozzle: 300 - 20 micron 0.8 mm nozzle: 600 - 20 micron
	XYZ resolution	6.9, 6.9, 2.5 micron
	Build speed	< 24 mm ³ /s
	Build plate	Heated glass build plate (20 - 140 °C)
	Nozzle diameter	0.4 mm (included) 0.25 mm, 0.6 mm, 0.8 mm (sold separately)
	Operating sound	< 50 dBA
	Connectivity	Wi-Fi, LAN, USB port
Physical dimensions	Dimensions (with Bowden tubes and spool holder)	495 x 585 x 780 mm (19.5 x 23 x 30.7 in)
	Net weight	20.6 kg (45.4 lbs)
Software	Supplied software	Ultimaker Cura, our free print preparation software Ultimaker Connect, our free printer management solution Ultimaker Cloud, enables remote printing
	Supported OS	MacOS, Windows, and Linux
Warranty	Warranty period	12 months

Figure 27. Ultimaker S5 Printer Information

While there are many different settings for 3D printing that can affect a print, not all need to be modified for this project. If the part experienced higher loads and there were more overhangs, more settings would be considered but in this case, the following six settings were optimized.

1. **Speed:** The amount of time it takes to produce a single layer of a 3D printed object. It is usually measured in millimeters per second (mm/s) or in cubic centimeters per minute (cc/min).
2. **Infill Pattern:** Refers to the structure that is used to fill the interior of a 3D printed object.
 - a. **Rectilinear:** a simple grid pattern that is easy to create and provides good stability and support.
 - b. **Triangular:** a pattern that resembles a honeycomb, and offers good strength and stability with a lower amount of material used.
 - c. **Concentric:** a circular pattern that can be used to achieve a specific aesthetic effect, but may not provide as much strength as other patterns.

- d. Random: a more complex pattern that is created by randomly distributing infill material throughout the interior of the object.
- 3. Infill Density: The amount of material used to fill the interior of a 3D printed object. Typically expressed as a percentage, with 100% meaning that the entire interior of the object is filled.
- 4. Supports: Structures added to the print body to provide stability and support during printing. Supports are especially important for complex models with overhanging or suspended parts that would otherwise collapse during the printing process.
 - a. Tree Supports: Tall, branching structures that look like tree branches. They are designed to provide support for large overhanging areas.
 - b. Lattice Supports: Grid-like structure added to the interior of an object to provide support. They offer good stability.
 - c. Linear Supports: Straight, pillar-like structures that are added to the object to provide support. They are typically used for simple objects with overhanging parts.
 - d. Breakaway Supports: Made of a material that can be easily broken or cut away from the object after printing is complete. They are often used for objects with complex geometries, and can be more difficult to remove than other types of supports.
 - e. Soluble Supports: Made of a material that dissolves in a chemical solution after printing is complete. They offer a convenient and effective way to support complex models, but require the use of a special solution and can be more time-consuming to remove.

5. Layer height: The thickness of each individual layer that is deposited during the printing process. Thicker layers result in faster printing times, but may produce coarser, less detailed prints. Thinner layers produce higher-quality, smoother prints, but take longer to print.
6. Shell thickness: The thickness of the outer layer or "shell" of a 3D printed object. Similar to infill density, the thicker the shell, the more rigid the part will be.

The last, and most important decision to be made was print orientation. Print orientation affects many aspects of a part including the following:

1. Strength and durability: Different orientations can affect the strength and durability of the final print. For example, printing with the objects' longest axis perpendicular to the build plate often results in a stronger print.
2. Overhangs and supports: The orientation of the object affects the likelihood of it having overhangs or needing supports. Minimizing overhangs and supports can help to improve the quality and speed of the print.
3. Warping: Some materials, particularly thermoplastics, are prone to warping as they cool and contract during printing. The orientation of the object can affect the likelihood of warping, with certain orientations being more prone to this issue.
4. Surface quality: The orientation of the object can affect the quality of the surface finish. Printing with the flat surfaces parallel to the build plate often results in a smoother surface.

The restrictor will be printed straight up from the bottom face that connects to the plenum. This was fairly obvious because it minimizes the amount of support needed and it also allows for the best resolution along the outer faces which is important for air flow. Luckily, this also provides the strongest print. Since the restrictor primarily experiences a distributed load in the form of wind, that force is pushing along the same axis as the print layers which is the strongest in 3D printing.

Since the plenum is slightly bent at the runners, it is not possible to print completely vertically. Therefore, the face of the plenum that connects to the runner portion of the plenum, will be orientated straight up. This will allow for the majority of the plenum to be printed vertically which is favorable in the same ways as it is for the restrictor. Since the start of the print will be angled, supports are necessary. The Ultimaker S5 has the option for supports made of the same print material like tree supports and also dissolvable supports. Since a clean surface finish, even on the outside is desirable, the dissolvable supports were chosen.

Manufacturing Phase - CNC Machining

The bottom portion of the runners, being made of 6061 aluminum, will be CNC milled. Machining as a manufacturing technique was used due to its ability to make the necessary complex geometries, tight tolerances, and relatively low invested time when compared to other potential methods such as casting. In order to make this component, Fusion 360's CAM software will be utilized to program the CNC milling machine at Lacy Hall. In an effort to reduce setup times, a 5 axis trunnion will be used, allowing us to access 5 sides of the part from one setup, greatly reducing manufacturing time. This part will get programmed using high efficiency milling techniques, in order to help reduce excess vibration due to thin part geometry.

The first step in the programming process is to identify difficult-to-machine geometry. For the runners the main two pieces of geometry which are difficult to make are the injector ports, and the throat of the runners themselves. By starting with the most difficult geometry, you're able to tailor the order of operations and the setup in order to make the most difficult parts easier. The steep injector angle will be solved through the use of the 5 axis trunnion which allows the part to be rotated to the necessary angle for machining without the use of an additional setup. The throat of the runners is an extremely complex shape, where the ellipsoidal port transitions up to a circle in the plenum with a 1 degree draft angle included inside of it. This is only possible to be made using 3D profiling techniques using extended reach ball nose end mills. Finally the part as a whole is extremely lightweight, and due to this and the workholding strategies used, is therefore extremely prone to chatter. Proper setup and fixturing will be used in order to dampen machining vibrations and reduce the chances of scrapping the part.

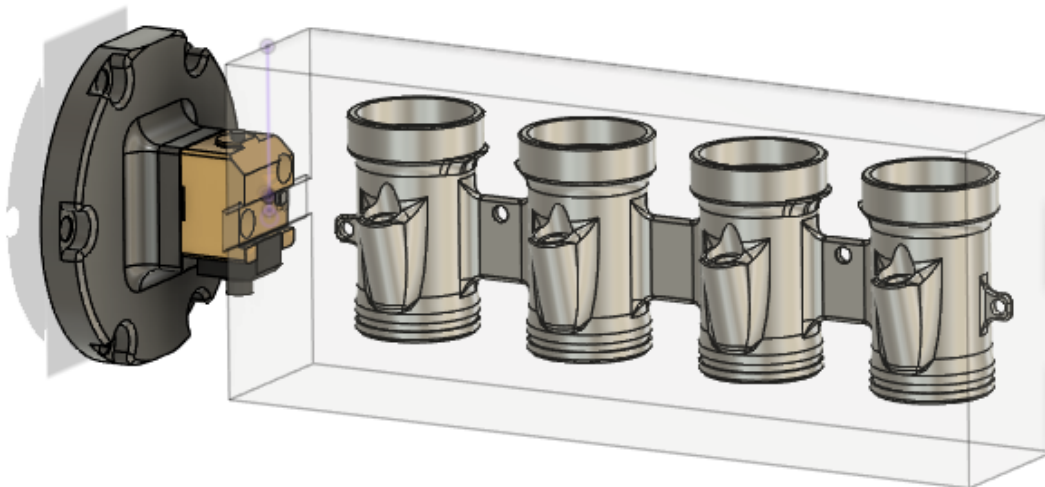


Figure 28: 5-Axis Machining Setup, Dovetail Vise and translucent raw material

To begin machining, the raw material is first waterjet in order to save excess material, allowing for other parts to be made using stock which would have otherwise been machined away. Then the stock or raw material needs to have a dovetail cut into it, this allows the 5 axis vise to hold onto the part and rotate it in space accurately using its locating pin, which gets machined to a tolerance of $\pm .0005''$. Once this is done the raw material can be loaded into the 5 axis trunnion table and the machining can begin.

The first steps are to remove large amounts of material from the tops and bottoms of the part. This allows for greater tool clearance as well as reducing the number of setups as these features can be finish machined in one operation. The roughing operations were done using heat shrink fit tool holding and high efficiency machining programming techniques in order to reduce the potential for vibration and tool chatter, which would cause part failure. After the outside of the part has been roughed, then the injector ports are bored and finish machined. Following these the external finishing passes with a ball nose end mill can occur, and finally the runner throat geometry mentioned above can be machined using an extended length $\frac{3}{4}''$ ball nose end mill.



Figure 29: Semi-finished runners in 5 axis trunion.

Manufacturing Phase - Epoxy Application

The 3D printing manufacturing process was an ideal method to create the restrictor and plenum due to their abnormal geometries and necessary material properties needed for all design parameters to be met. High quality 3D printers were used to obtain higher quality printed parts which includes reducing tolerancing errors and better surface finishes. However, even though the printed parts are relatively high in quality compared to if they were printed on less expensive machines, numerous surface defects were found on both the plenum and restrictor. These defects could potentially force air to deviate away from its path inside the parts and escape through them, reducing the overall power produced by the engine and its fuel efficiency. Defects from the 3D printing process include non-uniform wall thickness throughout certain sections and the unavoidable air gaps created as a result of the 3D printing process. 3D printing is an additive manufacturing process and as each layer gets deposited on top of the previous layer, there is a possibility of empty spaces forming between the layers. This can occur due to incomplete joining between layers which can be minimized with proper printing parameters. Leaving these airgaps in the print results in air escaping the intake system and decreasing the performance and efficiency of the engine. Thus, it is important to post-process these parts following the 3D-printing process which can be completed with a resin-based epoxy coating. The restrictor prior to and after applying two layers of epoxy resin to the surface can be seen in Figure 30. There were some protrusions of material that were thicker than the rest of the part that can be seen in (a) which were not ideal for our application. A total of 4 grams of epoxy was deposited onto the restrictor's surface and 80 grams on the plenum.



(a)



(b)

Figure 30. (a) Restrictor before epoxy coating; (b) Restrictor after epoxy coating

A step-by-step process for coating the restrictor and plenum to create an airtight coating is as follows:

- Wet-sand the part in circles starting with 600 grit sandpaper and work your way up to 1000 grit in increments of 200 grit. Once scratches and other imperfections start to get removed, move to a higher grit sandpaper and continue the same sanding process. Go slow and focus on not removing too much material while adding water to the surface when needed to remove some of the polycarbonate debris that will begin building up and to keep the sandpaper lubricated. Following the use of 1000 grit sandpaper, the surface of the part should be very smooth.
- Create the resin and hardener mixture using the metering pumps provided with the containers. The manufacturer states that a 3:1 ratio of resin to hardener is required

which is controlled with 1 pump of each (the metering pump is larger in the resin container which is how the ratio works out). Each pump extracts approximately 0.9 fluid ounces of each fluid.

- Pump each container three times into an empty container and vigorously mix it all together for about a minute.
- Once the mixture is mixed, attach a vacuum pump to the container to attempt to rid the mixture of air bubbles that formed while hand-mixing the mixture as shown in Figure 31. Also, tape up the inlets and outlets ports of the parts so that epoxy cannot drip inside.
- Take a paint brush (1" width was used), dip it into the mixture and begin applying the epoxy to the part as evenly as possible.
- Once the part is fully coated, take a heat gun and lightly apply it around the surface to remove any remaining air bubbles which can be seen in Figure 32.
- Set it to dry without touching the freshly coated surface. It will take about 24 hours for the epoxy to fully set and cure.
- Once dry, leak-test the part which is described in the *Assembly and Initial Testing* section.
- If more epoxy layers are required, repeat the process again starting with the second bullet point.



Figure 31. Vacuum Pump used to Remove Air from the Epoxy Mixture

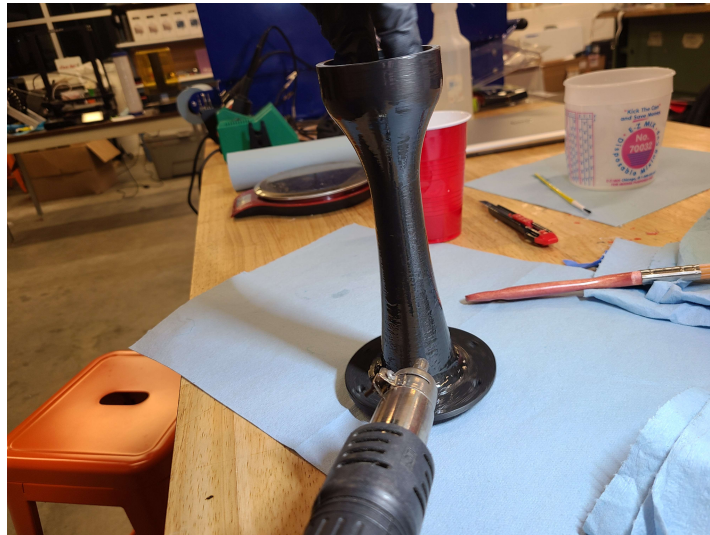


Figure 32. Heat Gun used to Remove Air Bubbles from Epoxy coating

Manufacturing Phase - Additional Components

1. Steel plate for uniform clamping force will be manufactured using a waterjet which is a machine that uses a high-pressure stream of water, mixed with an abrasive substance such as garnet, to cut materials such as metal, stone, glass, ceramics, and composites. The water is typically pressurized to 60,000 to 90,000 pounds per square inch (psi), producing

a powerful and precise cutting tool. The typical tolerance on the waterjet provided by the University varies based on material and cutting geometry but is estimated to be 0.007” in this case. Keeping this in mind, the hole size for the bolts will include an added tolerance to ensure clearance.

2. The same process as above will be used for the oil resistant Buna N Rubber sheet at the same connection since it has a simple 2D geometry.
3. Both the restrictor and plenum have additional structural and vibration damping supports that branch to either the engine (for the plenum) and chassis (for the restrictor). These supports consist of 3D printed brackets, thin aluminum plates, and p-clamps that will need to be manufactured using a variety of machines including a waterjet and manual mill.

Assembly and Initial Testing

Once all components were made, the assembly was ready to be assembled. Luckily, all components were designed with locating features which allowed for a simple and effective assembly process. Additionally all bolts were tightened with proper torque spec, and silicon hoses with hose clamps were used to secure the plenum to the runners. At this stage, the team decided to create rubber like caps to block all openings in the assembly to perform pressurized leak tests. This is a very important step in initial testing because if the assembly is not airtight, the intake will not be able to pull the ideal perfect vacuum. Leak tests were performed on the restrictor and plenum individually after each epoxy application and both were airtight with two coatings. Then all components were assembled and leak tested together to ensure all connections

were airtight. The full assembly was airtight after the first test which was a great improvement from last year.

Tuning

The final test of the intake system is tuning. One of the most crucial stages in the Formula SAE car's development is the first startup. Due to the large variety of moving parts, all of which needed to operate properly in order for the engine to function, this process can be very time consuming. After checking for leaks the intake system was installed onto the car. The intake sensors, Manifold air pressure (MAP), Throttle Position (TP), and Intake air temp (IAT) were all calibrated and verified to be working properly. These sensors then fed intake data to the engine control unit, which uses the data to control the car's running parameters, such as volumetric efficiency and ignition timing. Finally injection timing was verified as well as proper injector functionality in order to ensure proper operation.

The initial tuning process took only about 20 minutes to complete this year. This can be seen to be a huge improvement from last year which took several hours. This is in large part due to the high quality of the intake system manufactured this year. Properly functioning sensors allow for rapid tuning diagnosis, and the lack of intake leaks, which can be notoriously difficult to track down led to an extremely easy first startup for the team. The car was also able to idle at consistently lower RPMs than previous years, allowing for better fuel economy during event staging, as well as reduced noise levels from the exhaust which is measured at the competition.

Finally, the team will be headed to a chassis dynamometer in order to validate the intake design and finalize the tuning process. This will allow us to get accurate readouts on engine RPM, torque, and power curves, all extremely valuable empirical data to have when designing

for next year. Our volumetric efficiencies can be dialed in while at the dynamometer in order to optimize the air to fuel ratio which ensures a powerful but fuel efficient race car. Unfortunately the team wasn't able to find a shop that was compatible with the ECU being used until the last week of classes. Our initial power goals will not be validated in this report but we will be able to see the results before the 2023 competition.

Results/Conclusion

As the team comes to the end of the 2022-2023 season, there are many things that were accomplished, in both the intake and all other subteams of the car. The car is projected to not only perform better in dynamic events, but the engineers are also much more confident in presenting in front of the design judges this year due to the drastic increase in sophisticated engineering work and quantifiable designs and simulations. The completed intake system can be seen in Figure 33. While there were many accomplishments, the intake team also learned a lot as well. The following are improvements that can be made for years to come:

1. Be more prepared for 3D printing. With the plenum being so large and requiring a lot of material, as well as supports, a reliable printer that can print difficult materials like polycarbonate must be on hand.
2. Prepare ahead of time for all software needed to yield results. We were unable to access Ricardo Wave, a powerful engine simulation tool, which could have helped validate the intake runner lengths. We were also unable to perform vibrational analysis on the entire completed intake assembly in ANSYS because of the limitation on file size on the student version of the software.

While the team is not able to validate our initial goals for power and fuel efficiency at this time, we are eager to see these results in mid-May during the Formula SAE competition in Brooklyn, Michigan.

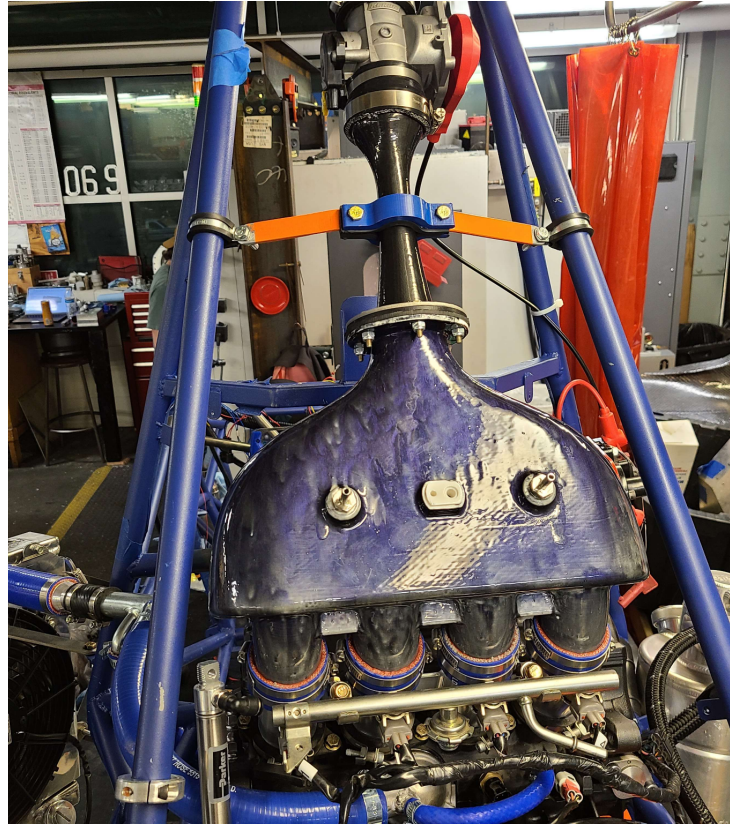


Figure 33. Intake assembled in car

This project will help our car be more fuel efficient and perform better which aligns with our clubs and the University's sustainability goals. Improving fuel efficiency and producing less emissions can help with many issues including

1. Reducing carbon dioxide emissions, nitrogen oxides, and particulate matter
2. Reduced dependency on fossil fuels

all of which help improve the state of the environment and improve human health. This project also was an incentive for other teams on the car to use more advanced computational methods

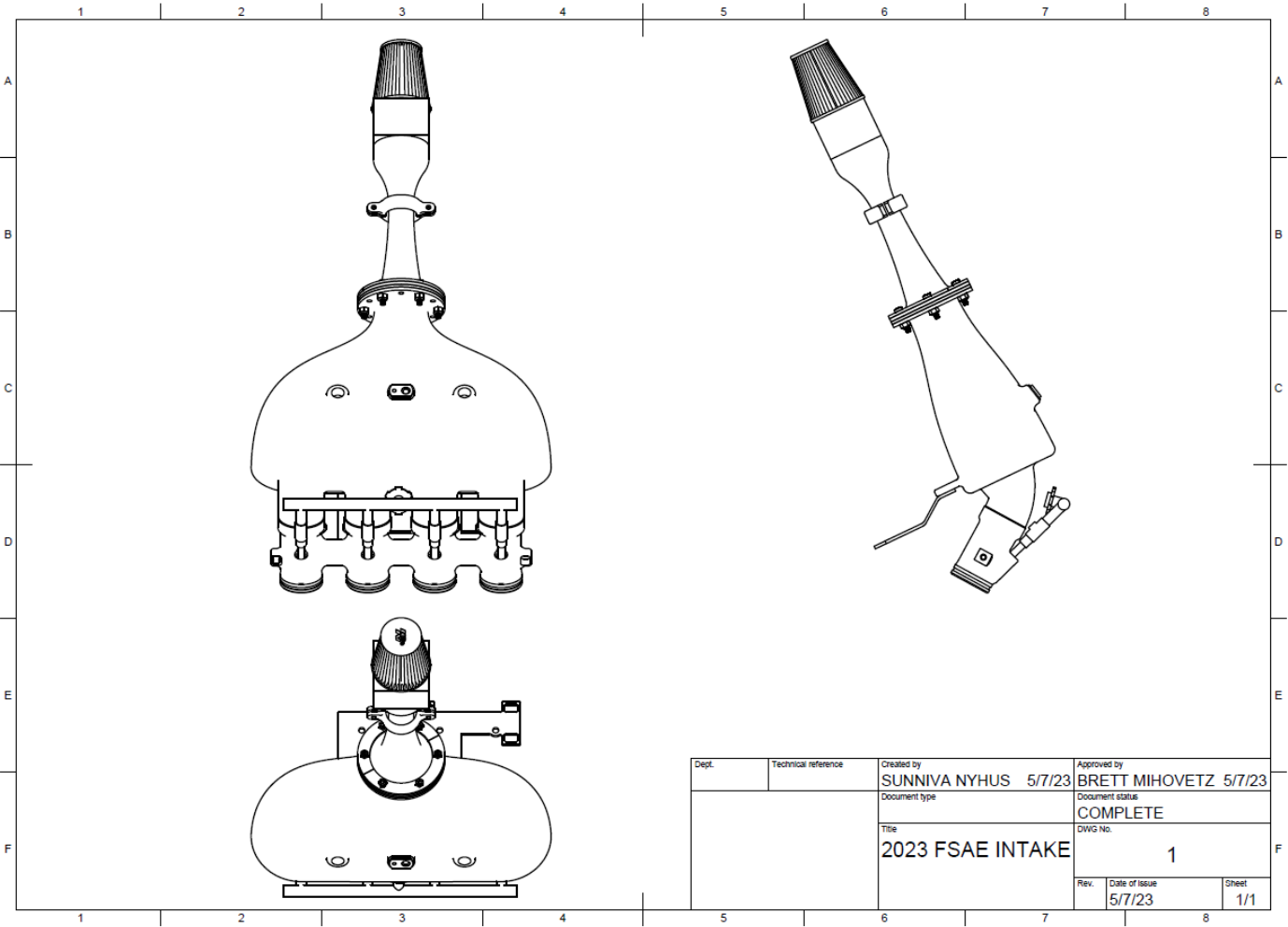
over just relying on hand calculations and physical testing, making us a more well rounded team in the eyes of design judges.

The cost of the overall assembly, including raw material, manufacturing costs, and all OEM parts is approximately \$942. This does not include the time taken to complete the design and manufacturing which would cost a company in a real life scenario. This cost also does not account for the cost of CNC milling the runners since Brett made those free of cost. Using the application Xometry, we estimate that the runners would cost around \$500 to make in a machine shop. At a large scale, this project could be simplified in terms of manufacturability to be more cost effective and time efficient.

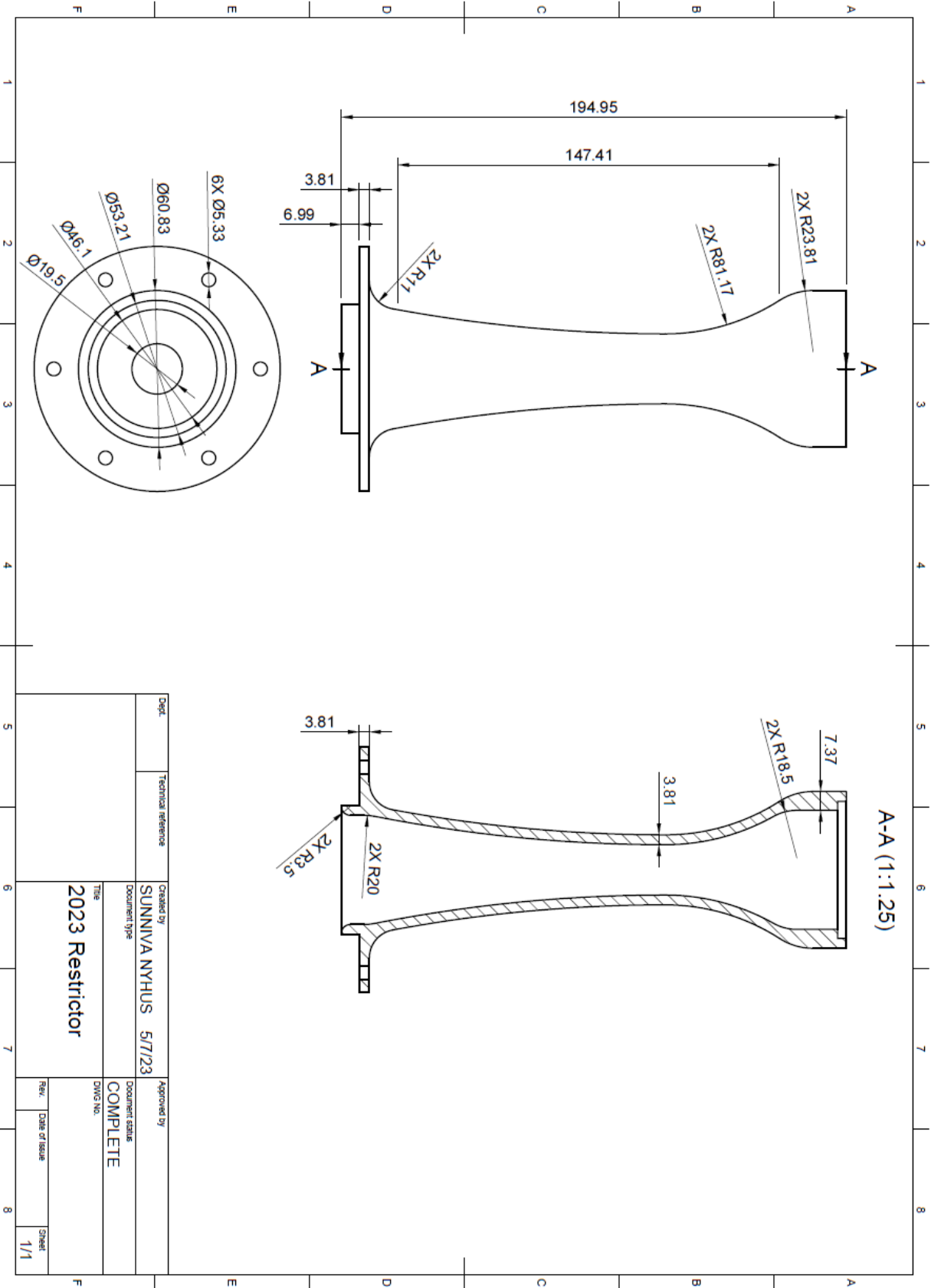
Appendix A: Bill of Materials

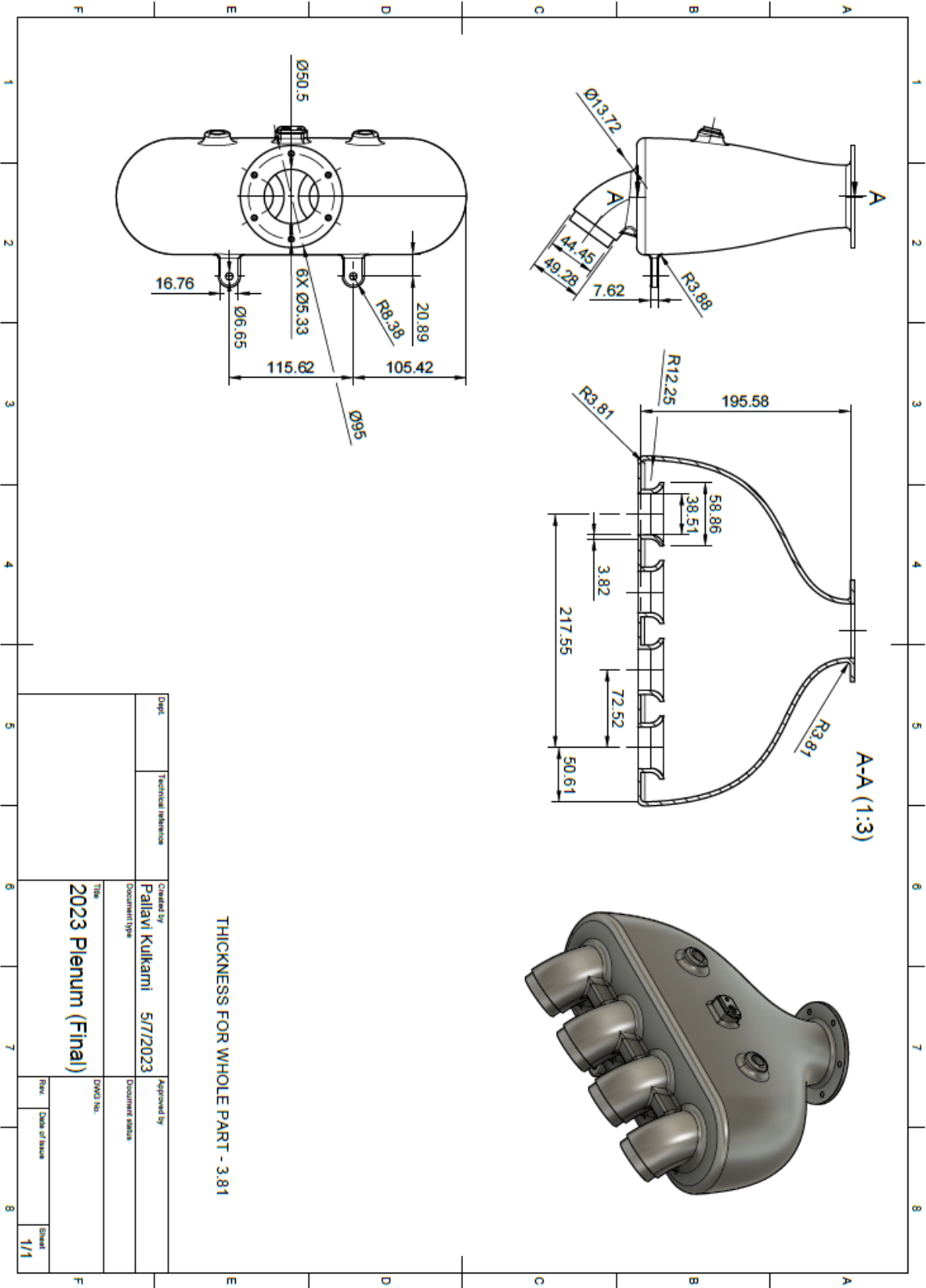
Part Number	Part Name	Quantity	Manufacturing Method	Cost (Student Pricing)	Cost (Regular Pricing)	Shipping Cost
1	Runners (base)	1	CNC Machined (YCM)	\$110.00	\$409.49	\$25.04
2	Plenum (and partial runners)	1	3D printed (Ultimaker S5)	\$0.00	\$318.00	\$24.67
3	Restrictor	1	3D printed (Stratasys F380)	\$0.00	\$134.00	\$24.67
4	Epoxy Resin	1	OEM	\$161.00	\$189.00	\$30.99
5	Gasket	1	OEM	\$11.69	\$11.69	\$10.24
6	Bolts	TBD	OEM	\$23.00	\$23.00	\$6.04
7	Nuts	TBD	OEM	\$5.44	\$5.44	\$5.99
8	Silicon Hose	1 ft.	OEM	\$14.69	\$14.69	\$9.00
9	Fuel Injectors	4	OEM	\$0.00	\$300.00	\$25.00

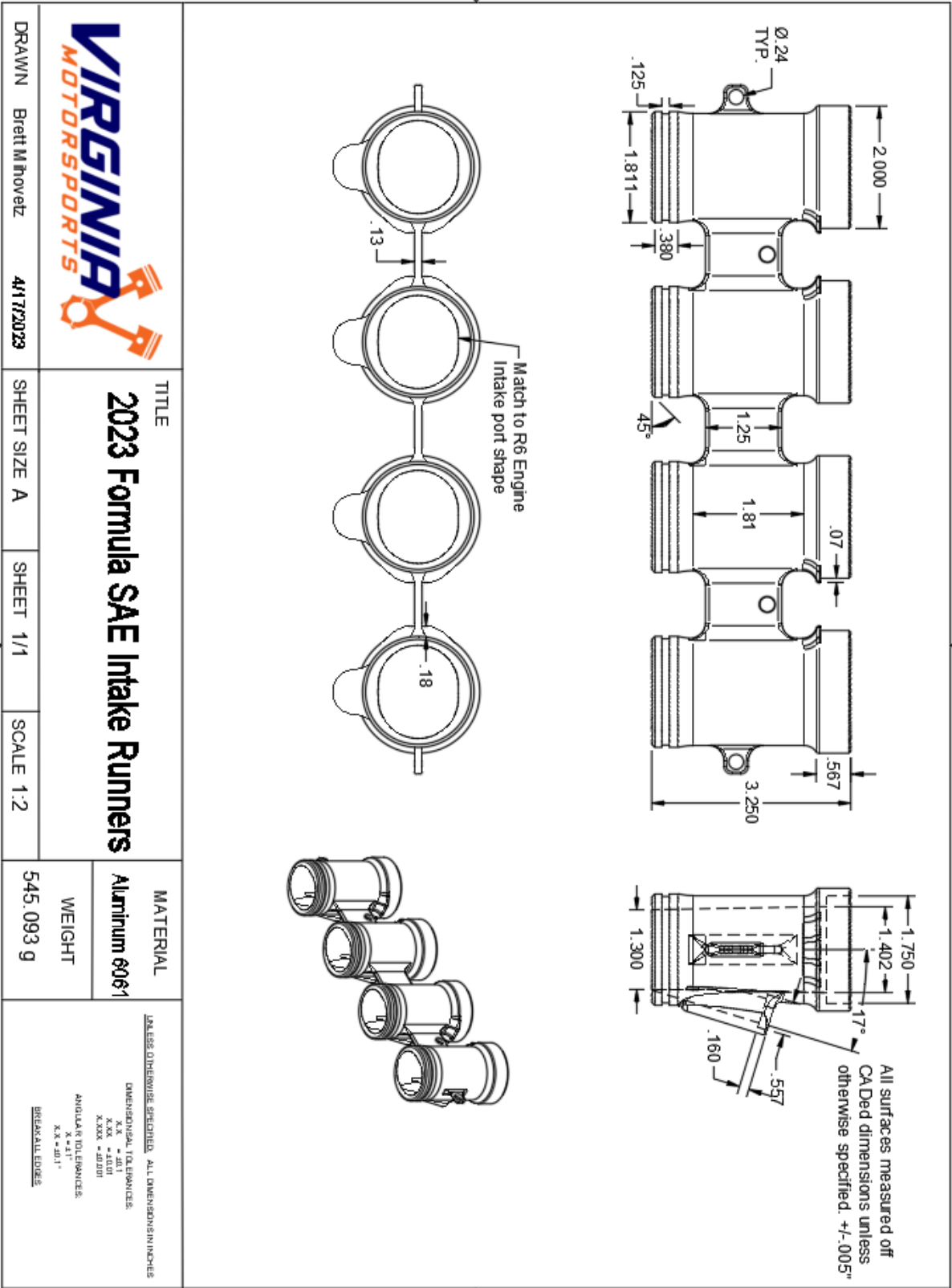
Appendix B: Assembly and Component Drawings



Dept.	Technical reference	Created by SUNNIVA NYHUS 5/7/23	Approved by BRETT MIHOVETZ 5/7/23
		Document type	Document status COMPLETE
		Title 2023 FSAE INTAKE	DWG No. 1
		Rev.	Date of issue 5/7/23
			Sheet 1/1

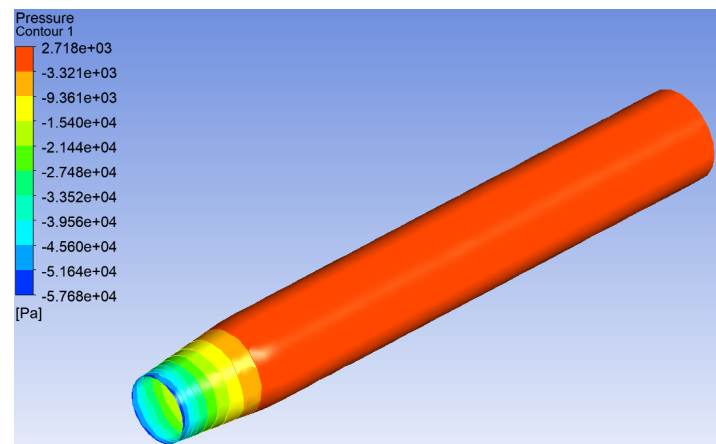
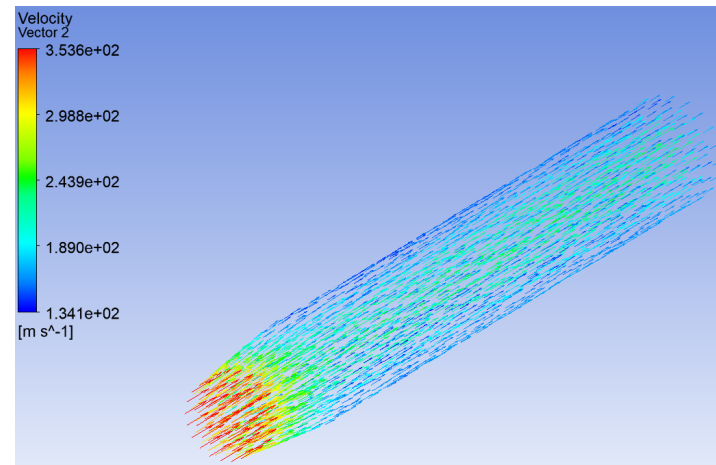
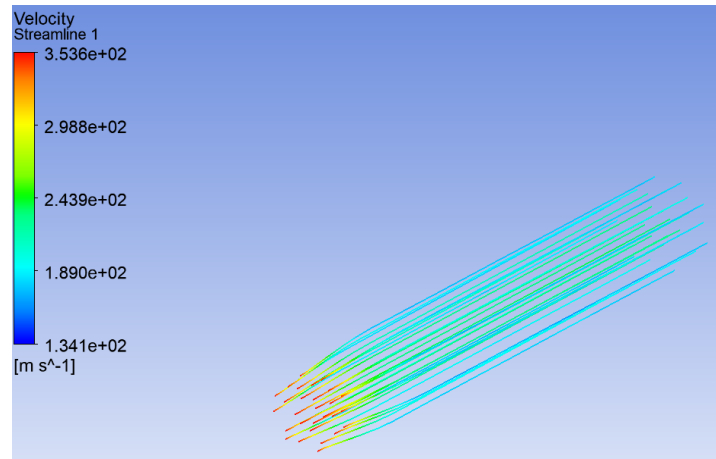




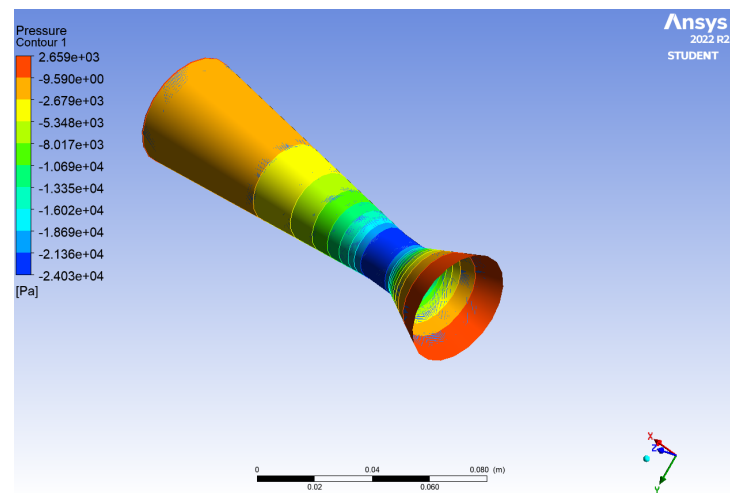
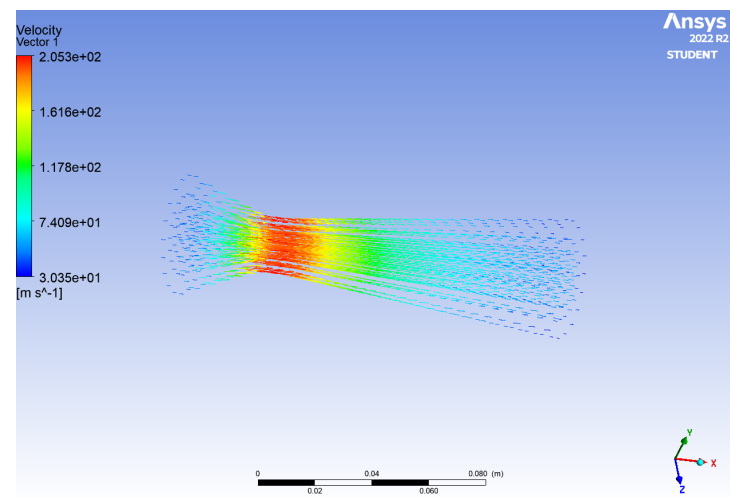
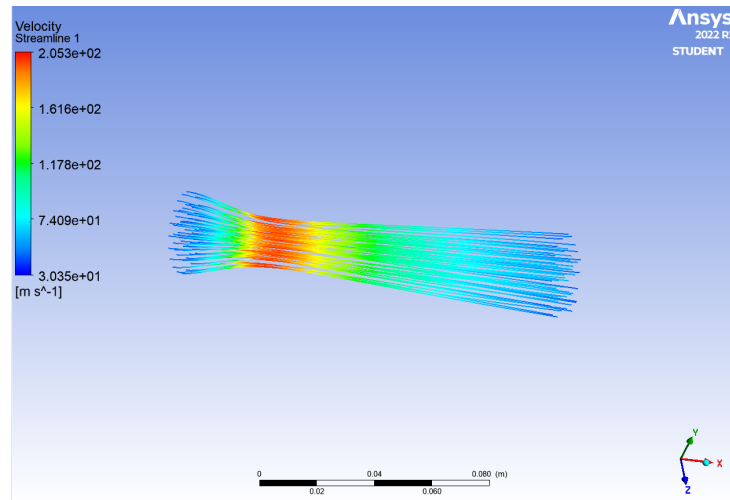


Appendix C: Restrictor Contour, Streamline, and Vector Results

No optimization Restrictor:

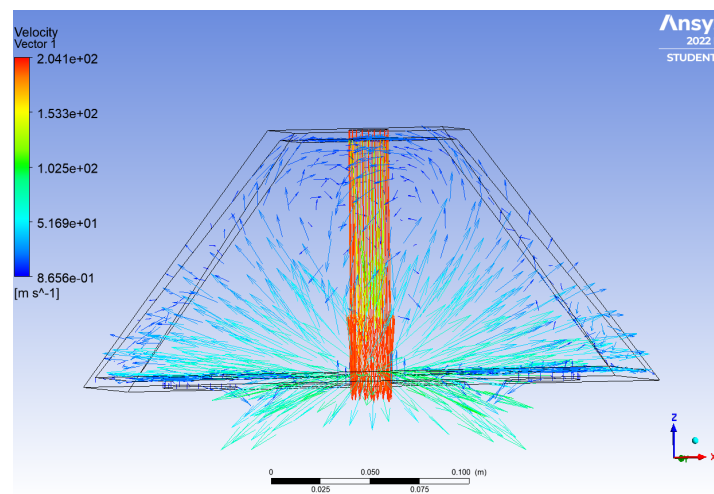
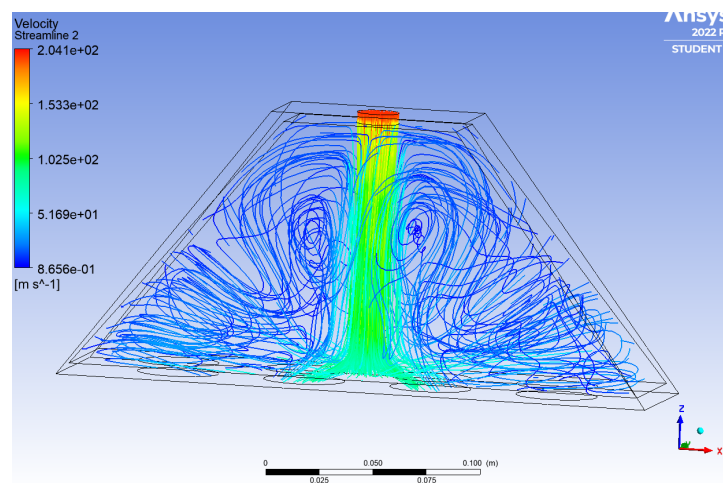
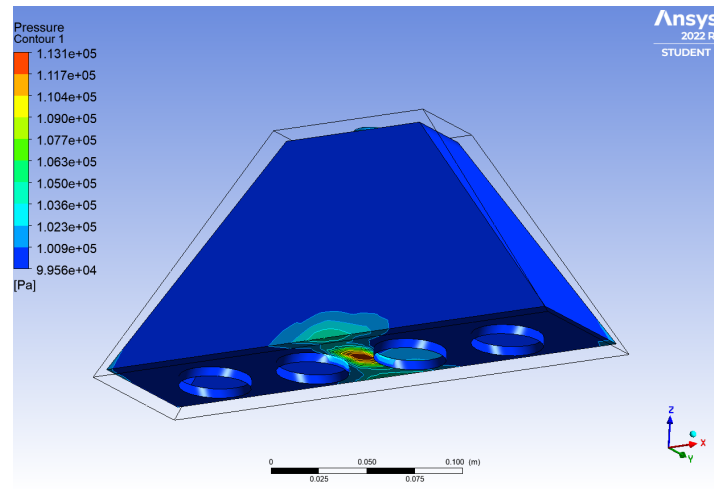


Optimized Venturi Restrictor:

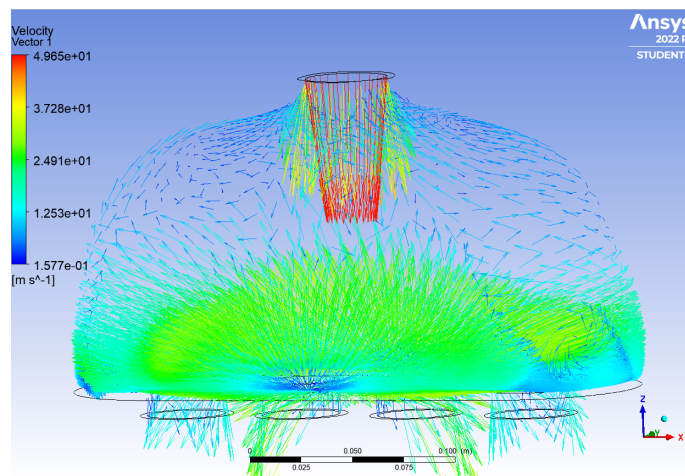
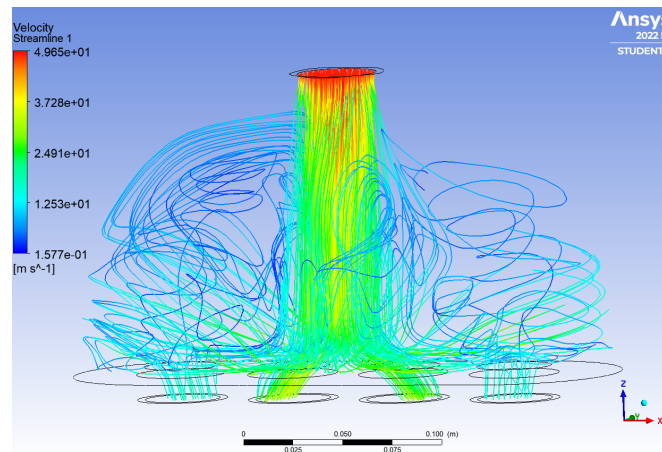
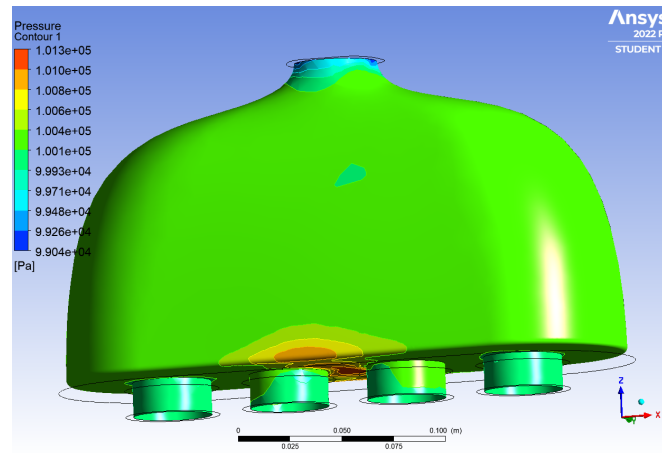


Appendix D: Plenum Contour, Streamline, and Vector Results

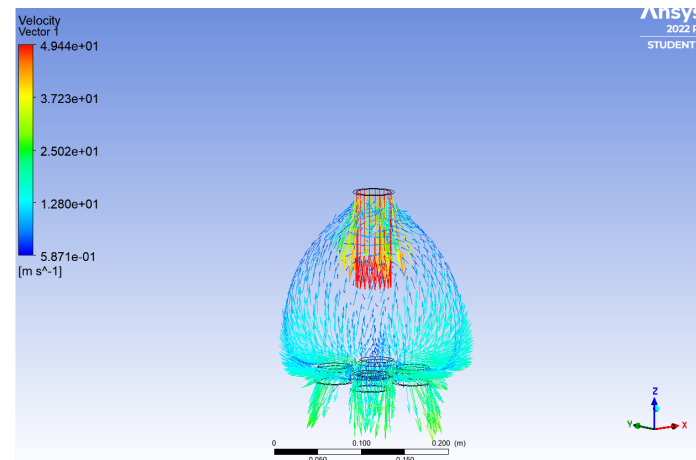
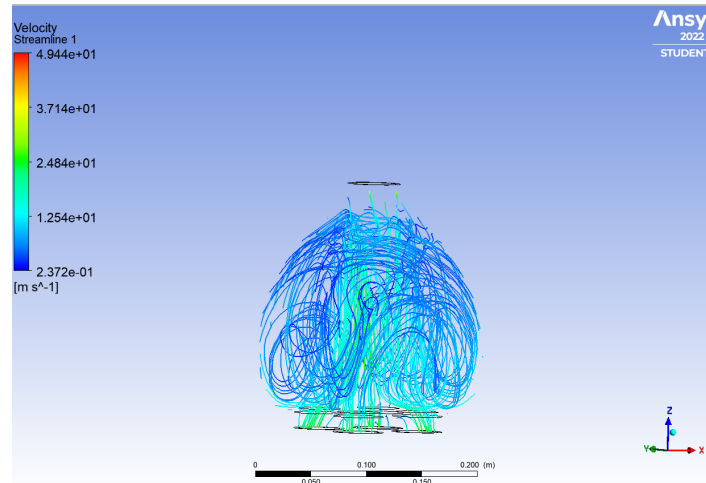
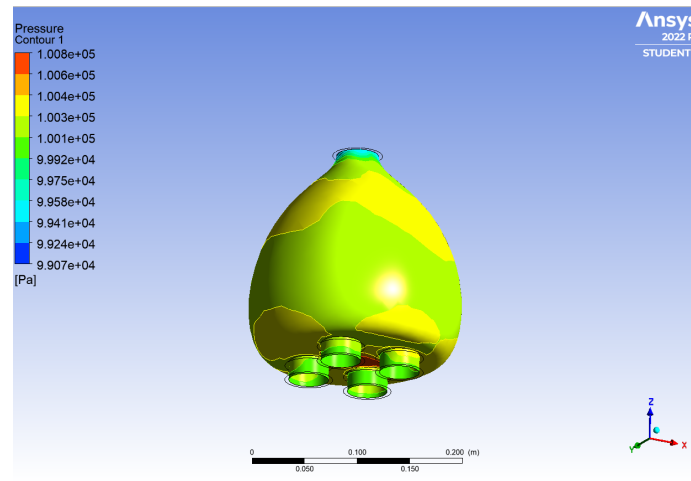
No optimization Plenum:



Plenum D1:



Plenum D2:



References

2019 FSAE Michigan Autocross Track. FSAEOnline.com. (n.d.). Retrieved November 15,

2022, from <https://www.fsaeonline.com/>

2019 FSAE Michigan Endurance Track. FSAEOnline.com. (n.d.). Retrieved November 15,

2022, from <https://www.fsaeonline.com/>

2023 FSAE rules V1. FSAE. (n.d.). Retrieved November 15, 2022, from

<https://www.fsaeonline.com/cdsweb/app/NewsItem.aspx?NewsItemID=b9717688-97c4-41f5-b386-74493aad0de6>

ANSYS, Inc. (2010, December). *Introduction to Ansys Fluent - iMechanica*. Introduction to CFD

Methodology. Retrieved November 29, 2022, from

https://imechanica.org/files/fluent_13.0_lecture08-udf.pdf

Epoxy Coatings Guide - A complete guide of epoxy coatings for industrial and marine

applications. The Sherwin Williams Company. (n.d.). Retrieved November 29, 2022,

from

<https://portlandgaragefloor.com/wp-content/uploads/2014/02/Epoxy-Coatings-Guide.pdf>

FSAE . (n.d.). *FSAE design score sheet 150PT*. FSAEOnline. Retrieved November 15,

2022, from <https://www.fsaeonline.com/content/FSAE%20Design%20Score%20Sheet-%20150pt.pdf>

Comprehensive guide on Acrylonitrile Butadiene Styrene (ABS). Acrylonitrile Butadiene Styrene

(ABS Plastic): Uses, Properties & Structure. (n.d.). Retrieved November 16, 2022, from <https://omnexus.specialchem.com/selection-guide/acrylonitrile-butadiene-styrene-abs-plastic>

Comprehensive guide on polycarbonate (PC). Polycarbonate (PC) - Properties, Uses, &

Structure - Guide. (n.d.). Retrieved November 16, 2022, from <https://omnexus.specialchem.com/selection-guide/polycarbonate-pc-plastic>

Gasket Pressure Guide. RAM Gasket Solutions. (2020, December 9). Retrieved December 12,

2022, from <https://www.ramgaskets.com/help/understanding-gasket-pressure/>

Hall, N. (Ed.). (2021, May 13). *Mass flow choking*. National Aeronautics and Space

Administration. Retrieved November 28, 2022, from <https://www.grc.nasa.gov/www/k-12/airplane/mflchk.html>

Markforged. (n.d.). *3D Printing Materials*. Markforged . Retrieved November 16, 2022, from

<https://markforged.com/resources/learn/3d-printing-basics/how-do-3d-printers-work/3d-printing-materials>

McMaster-Carr. (n.d.). Retrieved December 12, 2022, from

<https://www.mcmaster.com/sheet-gaskets/oil-resistant-buna-n-rubber-sheets-bars-and-strips/>

Munson, B. R., Okiishi, T. H., Huebsch, W. W., & Rothmayer, A. P. (2013). *Fundamentals of Fluid Mechanics* (7th ed.). John Wiley & Sons, Inc.

Momot, M. (n.d.). *Concept Selection. MAE 4610 Lecture 5.*

Overview of materials for Acrylonitrile Butadiene Styrene (ABS), Extruded. MatWeb Material

Property Data. (n.d.). Retrieved November 16, 2022, from

<https://www.matweb.com/search/DataSheet.aspx?MatGUID=3a8afcddac864d4b8f58d40570d2e5aa>

Overview of materials for nylon 12, carbon fiber filled. MatWeb Material Property Data. (n.d.).

Retrieved November 16, 2022, from

<https://www.matweb.com/search/DataSheet.aspx?MatGUID=70d79413fc04443b982cc34b5b161363>

Overview of materials for Polycarbonate, Extruded. MatWeb Material Property Data. (n.d.).

Retrieved November 16, 2022, from

<https://www.matweb.com/search/DataSheet.aspx?MatGUID=501acbb63cbc4f748faa7490884cdbca>

Shigley, J. E. (2007). *Mechanical engineering design*. McGraw-Hill Australia.

Taraborelli, P. (2022, July 30). *6 tips for choosing the best gasket – materials, types, uses.* Mercer

Gasket & Shim. Retrieved November 29, 2022, from

<https://mercergasket.com/6-tips-for-choosing-the-right-gasket/>

UC Components Inc. (2021, January 8). *Considerations for Selecting the Proper Fastener*

Materials for your Application. UC Components. Retrieved November 29, 2022, from

<https://www.ucomponents.com/considerations-for-selecting-the-proper-fastener-materials-for-your-application/>

Winterbone, D. E., & Pearson, R. J. (2001). *Design techniques for engine manifolds: Wave*

action methods for Ic engines. Society of Automotive Engineers.